NATIONAL ADVISORY COMMITTEE FOR AERONAUTICS

REPORT No. 319

AERODYNAMIC CHARACTERISTICS OF TWENTY-FOUR AIRFOILS AT HIGH SPEEDS

By L. J. BRIGGS and H. L. DRYDEN

UNITED STATES
GOVERNMENT PRINTING OFFICE
WASHINGTON : 1929

AERONAUTICAL SYMBOLS

1. FUNDAMENTAL AND DERIVED UNITS

	Symbol	Metric		English	
		Unit	Symbol	Unit	Symbol
Length	l	meter	m	foot (or mile)	ft. (or mi.)
Time	t	second	sec	second (or hour)	sec. (or hr.)
Force	F	weight of one kilogram	kg	weight of one pound	lb.
Power	P	kg/m/sec		horsepower	HP.
Speed		{km/hr		mi./hr	M. P. H.
		{m/sec		ft./sec	f. p. s.

2. GENERAL SYMBOLS, ETC.

W, Weight, $=mg$

g, Standard acceleration of gravity $=9.80665$ m/sec.$^2=32.1740$ ft./sec.^{2}

m, Mass, $=\frac{W}{g}$

ρ, Density (mass per unit volume).

Standard density of dry air, 0.12497 (kg-m^{-4} sec.^{2}) at 15° C and 760 mm $=0.002378$ (lb.-ft.$^{-4}$ sec.^{2}).

Specific weight of "standard" air, 1.2255 kg/m$^3=0.07651$ lb./ft.^{3}

mk^2, Moment of inertia (indicate axis of the radius of gyration, k, by proper subscript).

S, Area.

S_w, Wing area, etc.

G, Gap.

b, Span.

c, Chord length.

b/c, Aspect ratio.

f, Distance from $c.\ g.$ to elevator hinge.

μ, Coefficient of viscosity.

3. AERODYNAMICAL SYMBOLS

V, True air speed.

q, Dynamic (or impact) pressure $=\frac{1}{2}\rho V^2$

L, Lift, absolute coefficient $C_L=\frac{L}{qS}$

D, Drag, absolute coefficient $C_D=\frac{D}{qS}$

C, Cross-wind force, absolute coefficient $C_C=\frac{C}{qS}$

R, Resultant force. (Note that these coefficients are twice as large as the old coefficients L_C, D_C.)

i_w Angle of setting of wings (relative to thrust line).

i_t, Angle of stabilizer setting with reference to thrust line.

γ, Dihedral angle.

$\rho\frac{Vl}{\mu}$, Reynolds Number, where l is a linear dimension.

e. g., for a model airfoil 3 in. chord, 100 mi./hr. normal pressure, 0° C: 255,000 and at 15° C., 230,000;

or for a model of 10 cm chord 40 m/sec. corresponding numbers are 299,000 and 270,000.

C_p, Center of pressure coefficient (ratio of distance of $C.\ P.$ from leading edge to chord length).

β, Angle of stabilizer setting with reference to lower wing, $=(i_t-i_w)$.

α, Angle of attack.

ϵ, Angle of downwash.

REPORT No. 319

AERODYNAMIC CHARACTERISTICS OF TWENTY-FOUR AIRFOILS AT HIGH SPEEDS

By L. J. BRIGGS and H. L. DRYDEN
Bureau of Standards

40178—28——1

NATIONAL ADVISORY COMMITTEE FOR AERONAUTICS

NAVY BUILDING, WASHINGTON, D. C.

(An independent Government establishment, created by act of Congress approved March 3, 1915, for the supervision and direction of the scientific study of the problems of flight. It consists of 15 members who are appointed by the President, all of whom serve as such without compensation.)

REPORT No. 319

AERODYNAMIC CHARACTERISTICS OF TWENTY-FOUR AIRFOILS AT HIGH SPEEDS

By L. J. Briggs and H. L. Dryden

SUMMARY

The aerodynamic characteristics of 24 airfoils are given for speeds of 0.5, 0.65, 0.8, 0.95, and 1.08 times the speed of sound, as measured in an open-jet air stream 2 inches in diameter, using models of 1-inch chord. The 24 airfoils belong to four general groups. The first is the standard R. A. F. family in general use by the Army and Navy for propeller design, the members of the family differing only in thickness. This family is represented by nine members ranging in thickness from 0.04 to 0.20 inch. The second group consists of five members of the Clark Y family, the members of the family again differing only in thickness. The third group, comprising six members, is a second R. A. F. family in which the position of the maximum ordinate is varied. Combined with two members of the first R. A. F. family, this group represents a variation of maximum ordinate position from 30 to 60 per cent of the chord in two camber ratios, 0.08 and 0.16. The fourth group consists of three geometrical forms, a flat plate, a wedge, and a segment of a right circular cylinder. In addition one section used in the Reed metal propeller was included. These measurements form a part of a general program outlined at a conference on propeller research organized by the National Advisory Committee for Aeronautics and the work was carried out with the financial assistance of the committee.

INTRODUCTION

In Technical Report No. 207 of the National Advisory Committee for Aeronautics (Reference 1) an account is given of the results of some measurements by G. F. Hull and the authors of the aerodynamic characteristics of six airfoils of 3-inch chord in an open-jet air stream 12 inches in diameter at speeds from about 0.5 the speed of sound, to speeds in some instances approaching the speed of sound. The measurements supplemented those made by Caldwell and Fales at McCook Field (Reference 2), at speeds up to about 0.5 the speed of sound, confirmed the important influence of speed on the lift and drag coefficients, and established the following general relations:

1. The lift coefficient for a fixed angle of attack decreases rapidly as the speed increases.
2. The drag coefficient under the same conditions increases rapidly.
3. The center of pressure moves back toward the trailing edge.
4. The speed at which the rapid change in coefficients begins is decreased by (*a*) increasing the angle of attack and by (*b*) increasing the camber ratio.
5. The angle of zero lift shifts to higher negative angles up to the "critical" speed and then moves rapidly toward 0°.

These phenomena were further studied by measurements of the pressure distribution on models of 1-inch chord in a 2-inch air stream as described by the writers in Technical Report No. 255 (Reference 3) of the National Advisory Committee for Aeronautics. Speeds up to 1.08 times the speed of sound were obtained and it was shown that the large changes in the force coefficients were associated with a breaking away of the air flow from the upper surface, similar to that which occurs at the burble point at ordinary wind-tunnel speeds.

If a propeller is mounted directly on the shaft of a modern high-speed airplane engine, the outer airfoil sections of the propeller travel at speeds approaching the speed of sound. It is

possible by the use of gearing and a somewhat larger propeller to reduce the speed of the propeller sections, but only at the expense of additional weight and some frictional loss of power.[1] In order to determine whether gearing is desirable, it is necessary to know the loss of efficiency due to high tip speeds and to compare this loss with that due to the use of gearing. The problem is of increasing importance and at a conference on propeller research called by the National Advisory Committee for Aeronautics the Bureau of Standards was asked to determine the characteristics of the families of sections used by the Army and Navy in propeller design and such other sections as might be expected to lead to more efficient performance. This report presents the results of this work.

APPARATUS

Air stream.—The air stream was furnished by a duplex reciprocating compressor having a capacity of 1,800 cubic feet of free air per minute at gauge pressures up to 30 pounds per square inch. The air passed through three stabilizing tanks into a vertical pipe 8 inches in diameter, with a flow nozzle mounted at the upper end for forming the high-speed jet. The speed of the air stream was controlled and maintained constant by wasting air through blow-off valves on the stabilizing tanks. The values of the air speed were computed from the pressure observed on a manometer connected to a small hole in the 8-inch pipe about 1 foot ahead of the nozzle. Observations were taken at speeds of 0.5, 0.65, 0.8, 0.95, and 1.08 times the speed of sound at the temperature of the jet, corresponding to 563, 732, 902, 1,071, and 1,218 feet per second at 20° C.

Nozzles.—The two nozzles described in N. A. C. A. Technical Report No. 255 (Reference 3) were again used. A 2-inch cylindrical nozzle was employed for speeds below the speed of sound and a slightly expanding nozzle with a throat diameter of 1.9 inches and taper of 1 in 21 was used for the highest speed (1.08 times the speed of sound).

Airfoils.—The airfoils were 1 inch in chord and 6 inches long, and were mounted so as to span the air stream. The sections, Figures 6 to 45, may conveniently be considered as belonging to four groups. The first group may be termed the R. A. F. family and is based on one of the British R. A. F. sections (R. A. F. 6a). The members of the family differ only in thickness, all ordinates being increased in the same ratio, and are designated by a combination of numbers and letters such as 3R12. The R denotes that the family is derived from the R. A. F. section; the first number 3 denotes the position of the maximum ordinate in tenths of the chord length, and the second number denotes the camber ratio (or thickness ratio since the lower surface is plane) in hundredths of the chord length. Six members of the family, namely, 3R10, 3R12, 3R14, 3R16, 3R18, and 3R20 are the sections used in the tests described in N. A. C. A. Technical Reports Nos. 207 and 255 (References 1 and 3), referred to there as airfoils 1, 2, 3, 4, 5, and 6.[2] In the present work 3R4, 3R6, and 3R8 were included with the six already referred to, making a total of nine members in the family.[2]

The second group was of the same type except that a Clark Y section was used as the basic section. Five members of the family were represented in the tests, namely, C4, C8, C12, C16, and C20. The maximum ordinate designation is omitted since no additional C sections were tested.

The third group consisted of two subgroups, both derived from the R section. The primary variable was the position of the maximum ordinate and the subgroups correspond to two camber ratios. In the above designation the additional sections were 4R8, 5R8, 6R8, 4R16, 5R16, and 6R16. Two members of the first family, namely, 3R8 and 3R16, may also be considered in this third family.

The fourth group consisted of four sections belonging to none of the preceding families. A flat plate with the ratio of thickness to chord equal to 0.04, a wedge with the base thickness equal to 0.08 times the chord, a circular arc of camber ratio equal to 0.08, and a section repre-

---

[1] It is common practice to increase propeller efficiency by using reduction gear to secure aerodynamic advantage.

[2] The same sections are designated as U. S. N. P. S. sections in Technical Report No. 259 of the National Advisory Committee for Aeronautics (Reference 4), and carry different numbers, 3R10 or 1 corresponding to U. S. N. P. S. 3, 3R12 or 2 to U. S. N. P. S. 4, 3R16 or 4 to U. S. N. P. S. 5, and 3R20 or 6 to U. S. N. P. S. 6. U. S. N. P. S. 1 and U. S. N. P. S. 2 correspond to 3R4 and 3R8 in our new designation.

sentative of those used in the Reed metal propeller were included. All of these special sections had a chord of 1 inch.

The nominal ordinates of the sections are shown in Table I. The airfoils were made by W. H. Nichols, of Waltham, Mass., and check measurements showed that the departures from the nominal ordinates did not exceed 0.001 inch and were usually much less.

BALANCE.—The balance used for the force measurements is shown in Figure 1 and the airfoil mounting alone in Figure 2. The diagramatic sketch in Figure 3 gives a somewhat better illustration of the operation. The airfoil is held in a fork A, which is rotatable (about a longitudinal axis in the airfoil) by means of a worm and gear with respect to a second fork B, which is rigidly attached to a post C hung from the beam of the drag balance D. The lift force is transmitted by the parallel linkage E to the drag balance support F, the joints of the linkage being made by thin flexible strips G. The drag force is balanced by means of weights on a scalepan H, a rider I, and finally by a chain J hung from the end of the beam and from a graduated wheel K. The zero position of the drag beam is indicated by a level L on the lower member of the linkage E.

The drag balance is supported by one member M of the lift linkage, which is in the form of a parallelogram with ball bearings N at the four corners. One arm of the linkage carries a lever O which transmits the lift force to the platform of the lift balance P. Suitable counterweights and damping devices are provided, and the whole mechanism is mounted on sliding ways so that the airfoil can be removed from the stream and be replaced by another without stopping the air stream. Lift and drag measurements may be made independently and simultaneously.

REDUCTION OF OBSERVATIONS.—In N. A. C. A. Technical Report No. 255 (Reference 3) we have given at some length the method of computing the air speed and the velocity pressure, $\frac{1}{2}\rho V^2$. Consequently, we repeat only the notation and the final equations.

NOTATION

p_i = absolute static pressure inside pipe (velocity pressure negligible).
p_o = absolute static pressure in jet (equal to barometric pressure).
$p_i - p_o$ = impact pressure.
V = speed of air in jet.
c = speed of sound at temperature of jet.
c_o = speed of sound at 0° C.
ρ = density of air in jet.
$q = \frac{1}{2}\rho V^2$ = velocity pressure.
J = mechanical equivalent of heat.
C_p = specific heat of air at constant pressure.
k = ratio of specific heats.
C_L = lift coefficient.
C_D = drag coefficient.
A = area of airfoil taken as chord times exit diameter of nozzle.
L = lift.
D = drag.

The following relations are derived in N. A. C. A. Technical Report No. 255 (Reference 3):

$$\frac{V^2}{c^2} = \frac{546 J C_p}{c_o^2} \left\{ \left(\frac{p_i}{p_o} \right)^{\frac{k-1}{k}} - 1 \right\}$$

$$\frac{1}{2}\rho V^2 = \frac{288 \times 0.0012255}{1013300} J C_p p_o \left\{ \left(\frac{p_i}{p_o} \right)^{\frac{k-1}{k}} - 1 \right\}$$

$$\frac{p_i - p_o}{\frac{1}{2}\rho V^2} = \frac{(1 + 0.19991\, V^2/c^2)^{7/2} - 1}{3.5088 \times 0.19991\, V^2/c^2}$$

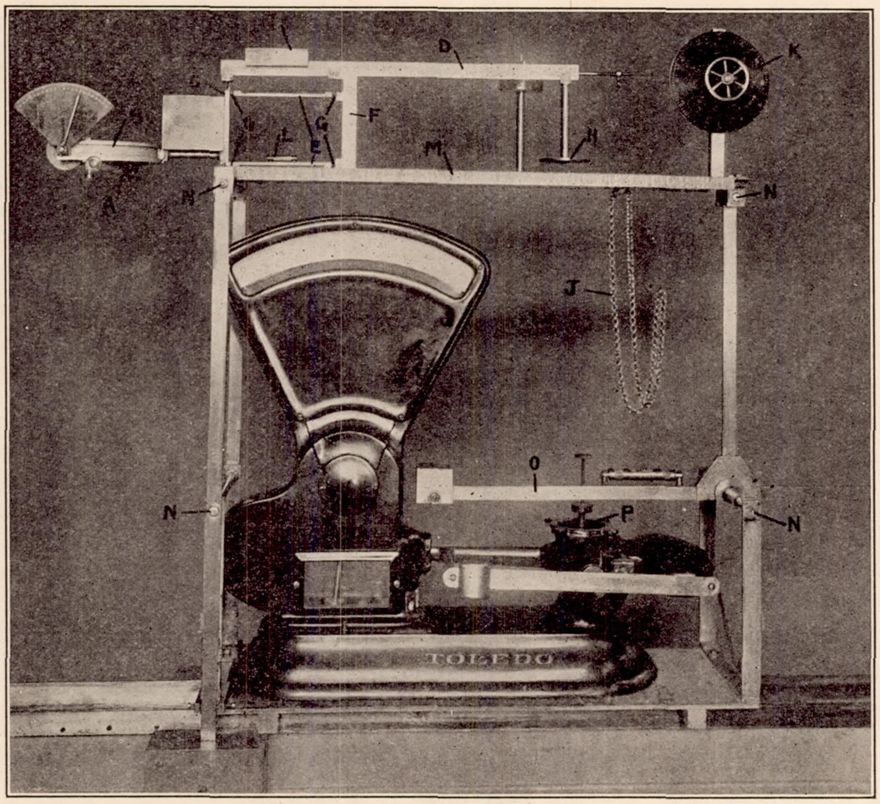

FIGURE 1.—The balance

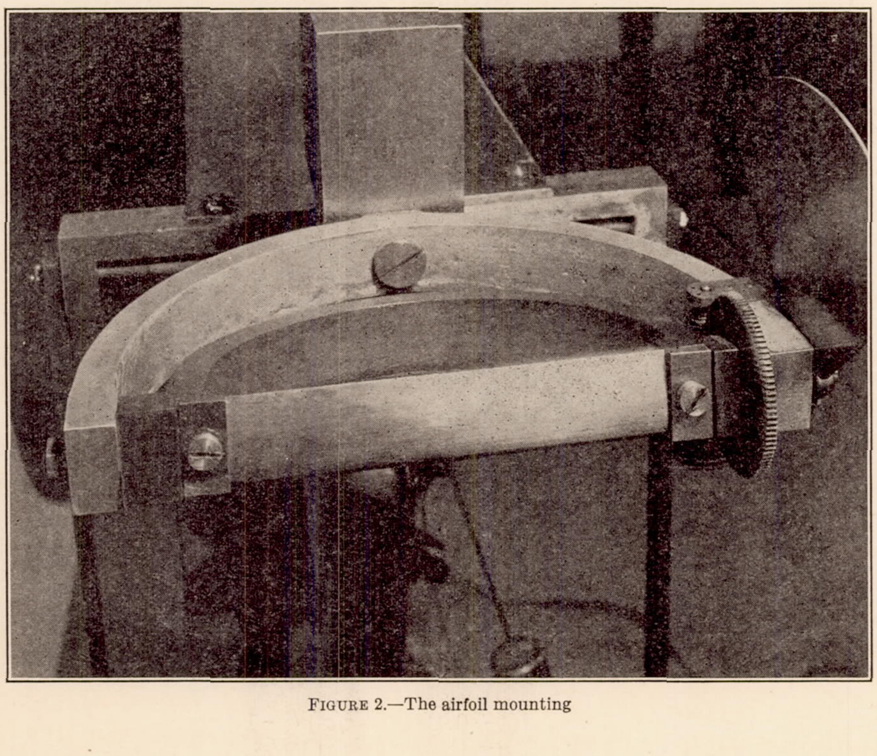

FIGURE 2.—The airfoil mounting

The lift and drag coefficients are defined by the equations:

$$C_L = \frac{L}{\frac{1}{2}\rho V^2 A}$$

$$C_D = \frac{D}{\frac{1}{2}\rho V^2 A}$$

The quantities V/c, C_L, and C_D were computed from the observed lift, drag, pressure inside the pipe, and the barometric pressure by means of these equations.

RESULTS.—The results are given in the form of polar diagrams in Figures 6 to 14, 21 to 25, 31 to 36, and 42 to 45, inclusive, and comparison between members of the same family is facilitated by the cross-plots of drag coefficient against camber ratio for various lift coefficients given

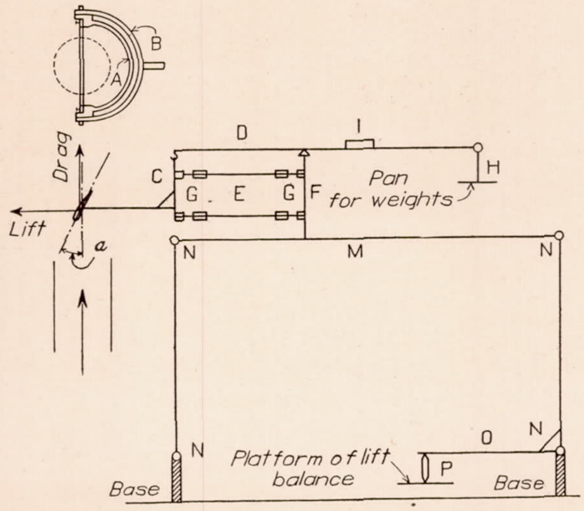

FIGURE 3.—Diagrammatic sketch of airfoil balance

in Figures 16 to 20 and 26 to 30. The data for the most useful range of angles from $-4°$ to $+20°$ are also given in tabular form in Table II.

As an experiment in visual representation, Figures 4 and 5 are photographs of a three-dimensional model giving the results for one airfoil. One pair of axes correspond to the usual C_L and C_D axes of the polar diagram, and sections parallel to the plane of these axes are polar diagrams. The third axis is that of V/c. The main characteristic of the surface is a hillside slope running diagonally across the model connecting two fairly level plateaus. The higher plateau (to the right in the photographs) represents the region of smooth flow and the lower (to the left) the high-speed burbling type of flow. The diagonal trend of the slope shows that at the higher lift coefficients, the change of flow begins at a lower speed.

EFFECT OF POSITION OF AIRFOIL IN AIR STREAM

The measurements given in this report were made with the center of the airfoils at a distance of 5 centimeters from the plane of the mouth of the nozzle. A number of measurements were made at other positions, namely, 2.7 centimeters above and 10 centimeters above. It was found that so long as the flow was smooth no appreciable effect of position was found. When, however, the flow breaks away from the surface as at high speeds or with thick sections, systematic effects are present. The greater part of the effect can be described by saying that the forces behave as if the absolute pressure in the "dead water" region decreased as the distance of the airfoil from the plane of the nozzle mouth was increased. The changes amounted to 0.04 in the lift coefficient and to 0.008 in the drag coefficient at a given angle of attack for the thickest sections at the two higher speeds; that is, in the worst cases.

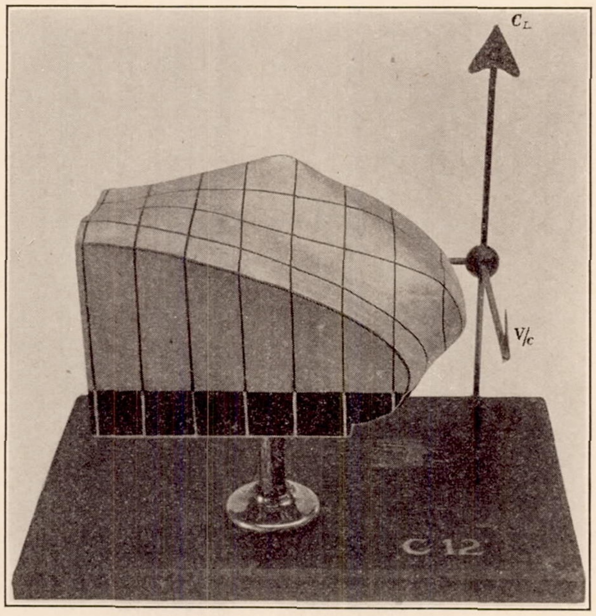

FIGURE 4.—Solid model illustrating relationship between C_L, C_D, and V/c

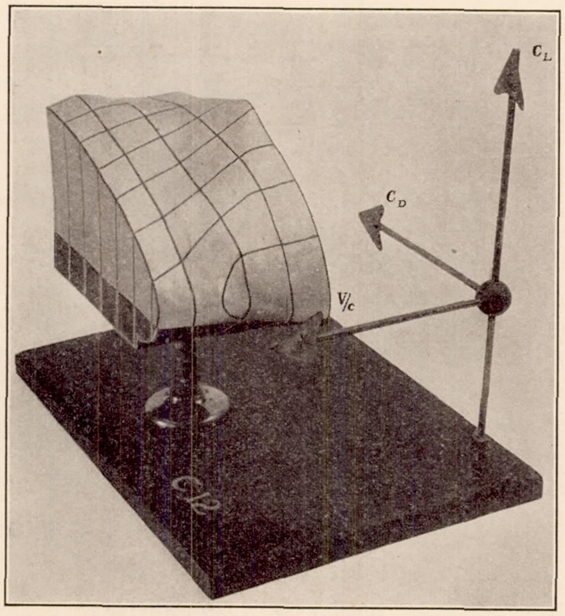

FIGURE 5.—Solid model illustrating relationship between C_L, C_D, and V/c

40178—29——2

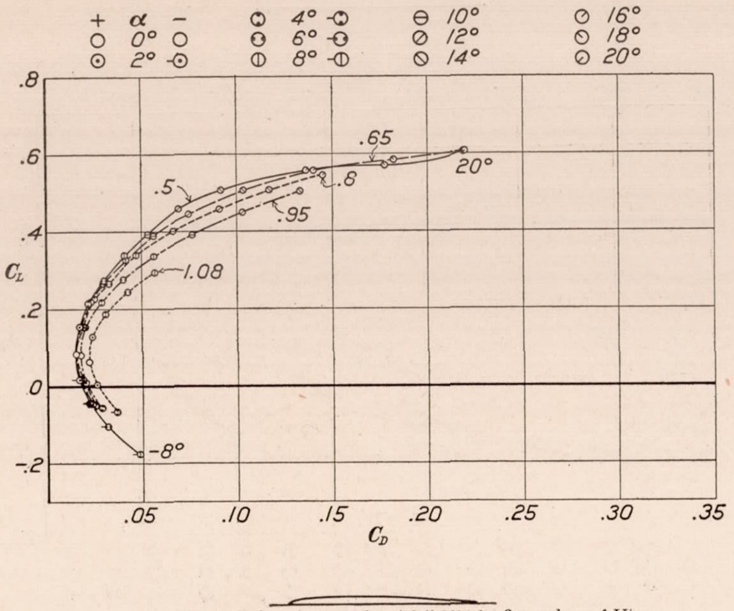

FIGURE 6.—Polar diagrams for airfoil 3R4 for five values of V/c

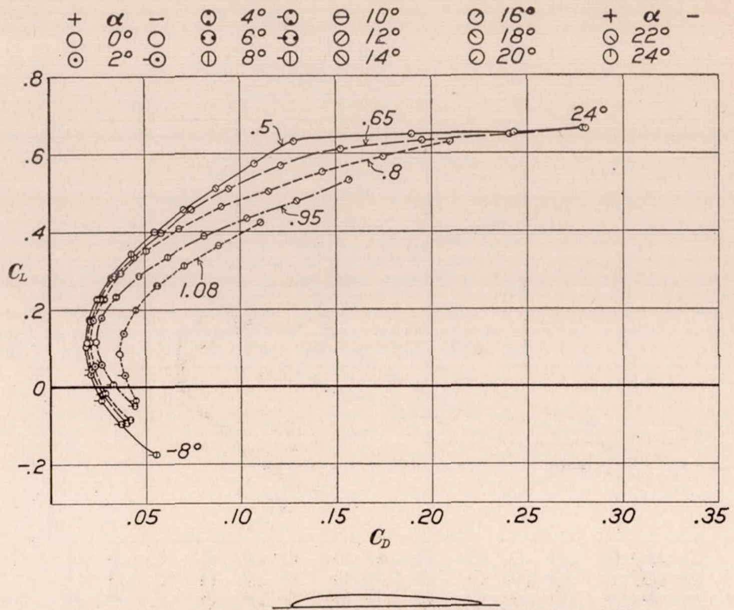

FIGURE 7.—Polar diagrams for airfoil 3R6 for five values of V/c

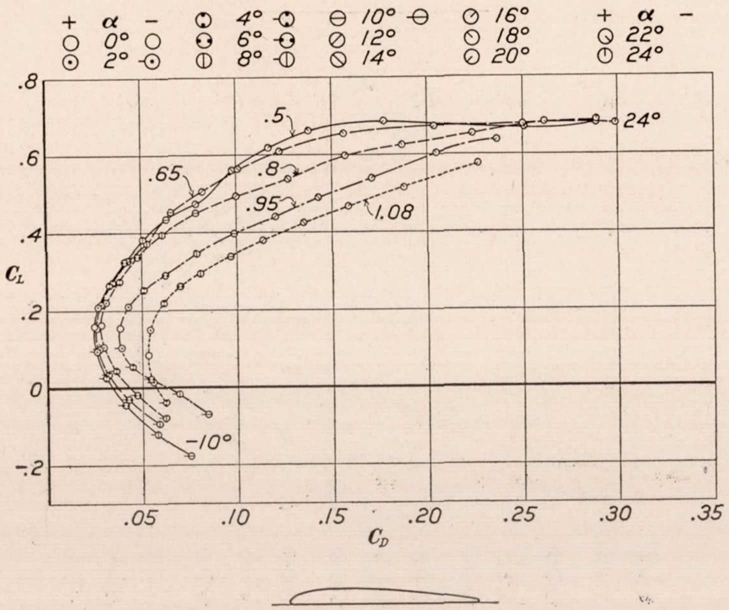

FIGURE 8.—Polar diagrams for airfoil 3R8 for five values of V/c

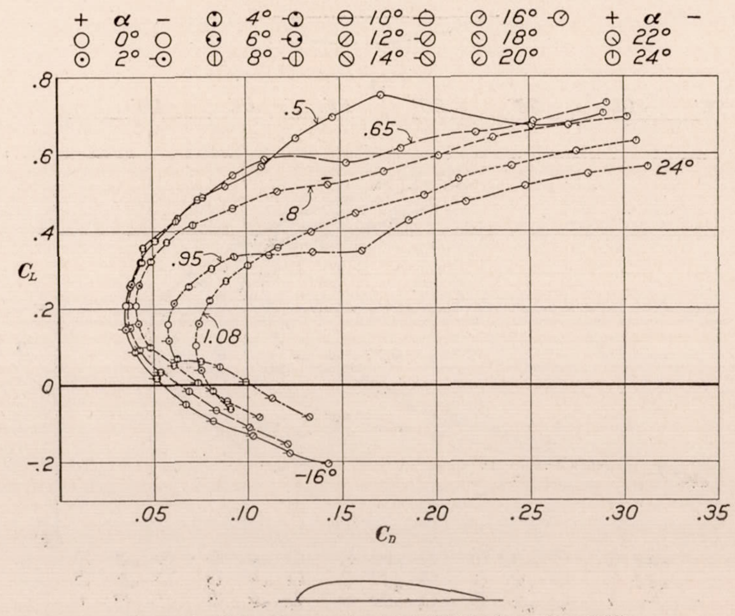

FIGURE 9.—Polar diagrams for airfoil 3R10 for five values of V/c

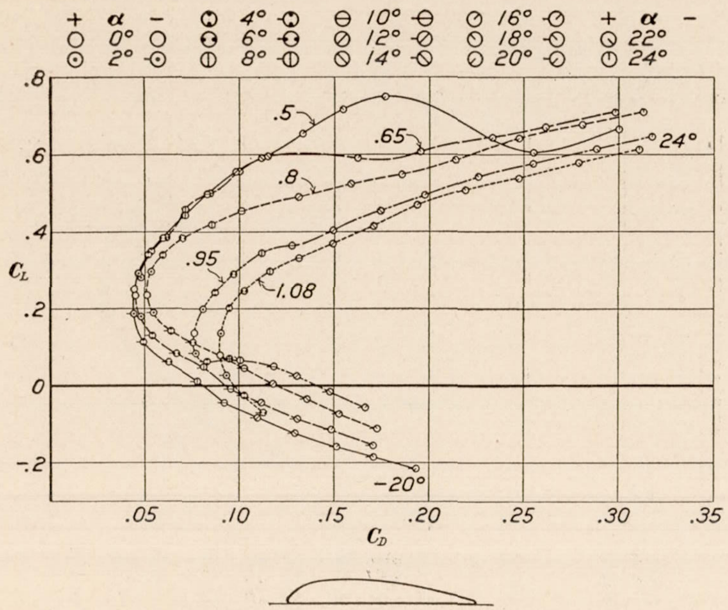

FIGURE 10.—Polar diagrams for airfoil 3R12 for five values of V/c

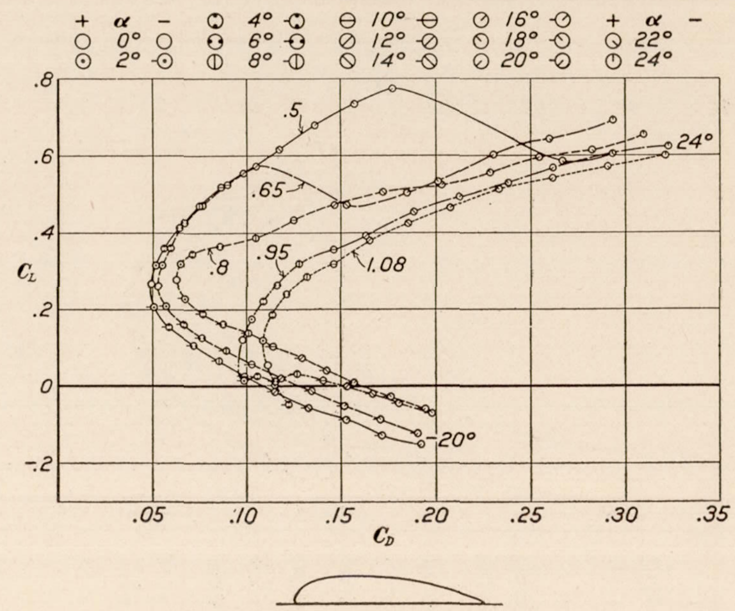

FIGURE 11.—Polar diagrams for airfoil 3R14 for five values of V/c

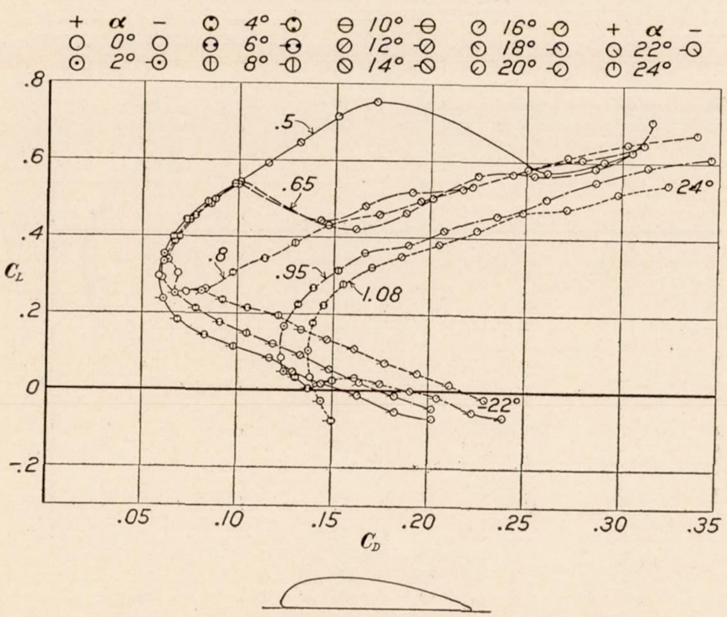

FIGURE 12.—Polar diagrams for airfoil 3R16 for five values of V/c

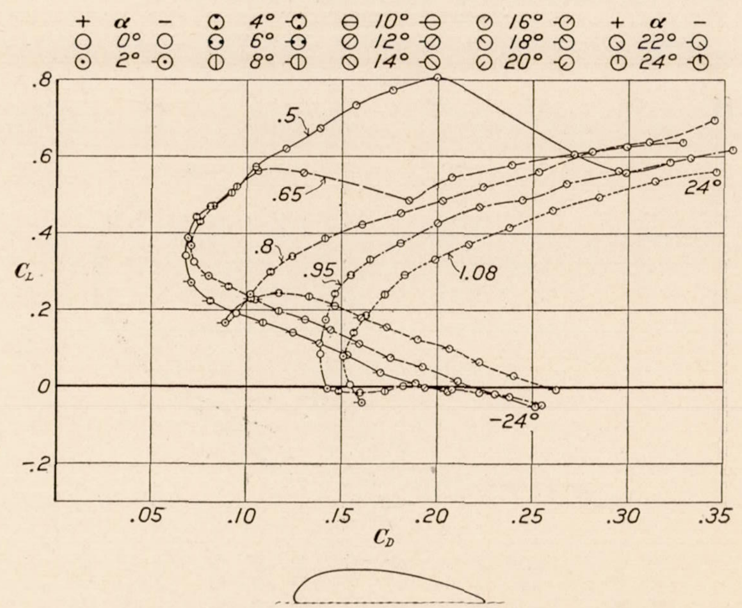

FIGURE 13.—Polar diagrams for airfoil 3R18 for five values of V/c

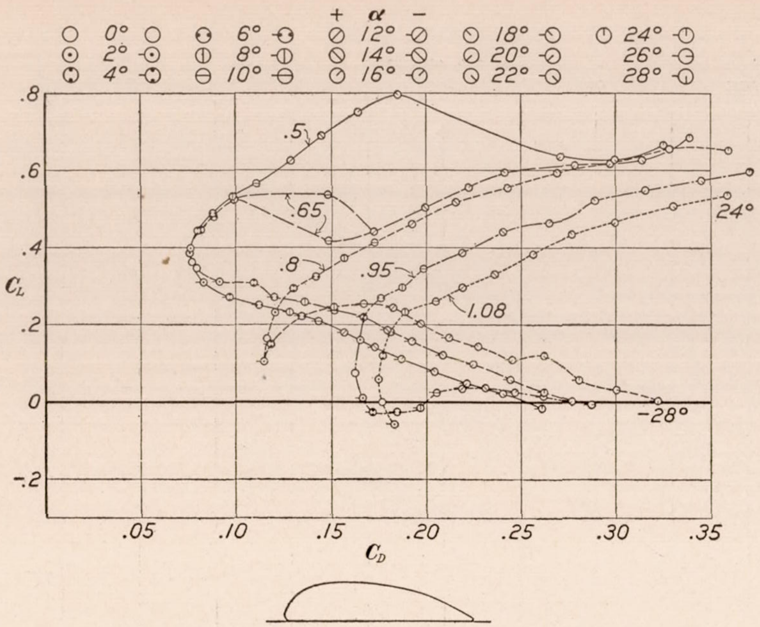

FIGURE 14.—Polar diagrams for airfoil 3R20 for five values of V/c

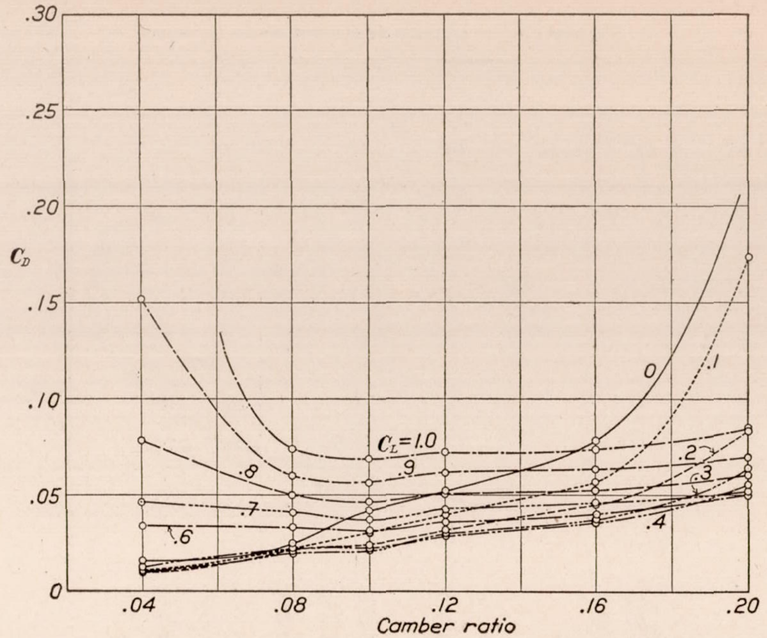

FIGURE 15.—Drag coefficient, C_D vs. camber ratio for various lift coefficients, C_L, at V/c=0.05, for 3R family

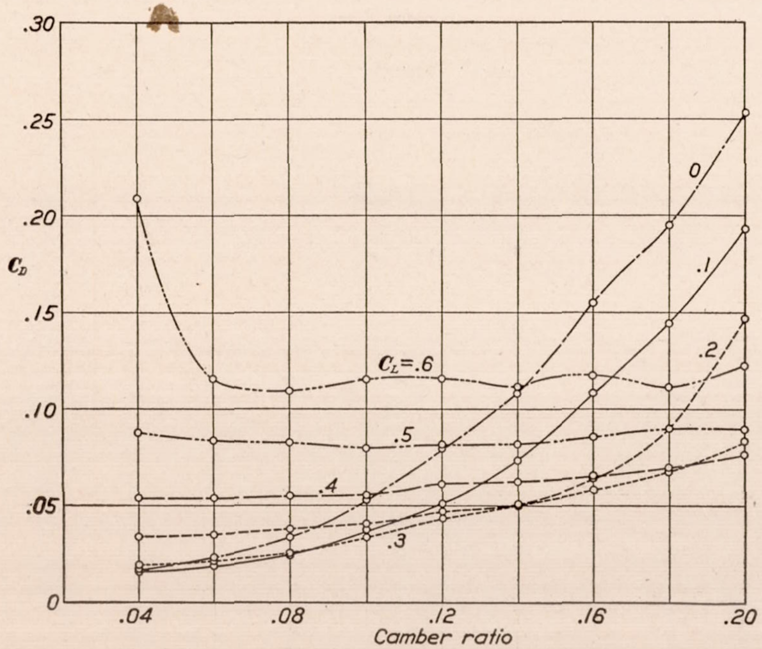

FIGURE 16.—Drag coefficient, C_D vs. camber ratio for various lift coefficients, C_L, at V/c=0.50, for 3R family

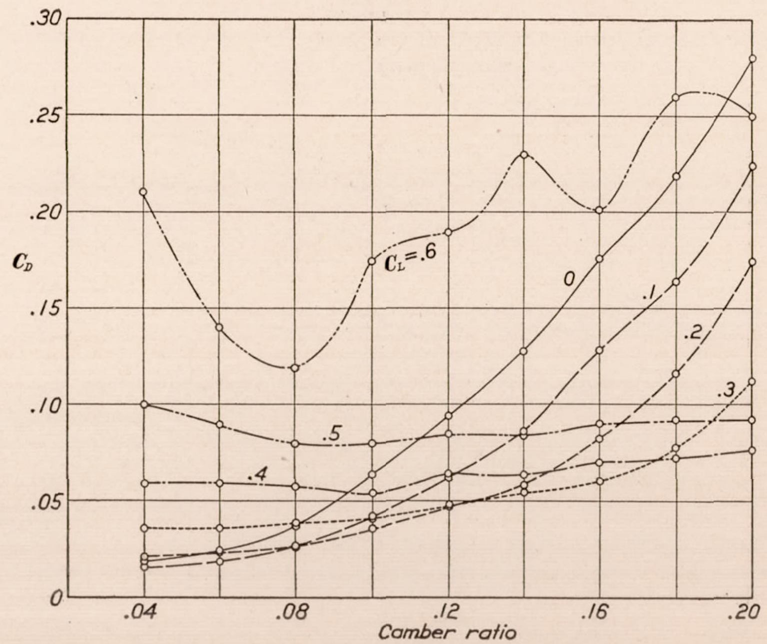

FIGURE 17.—Drag coefficient, C_D vs. camber ratio for various lift coefficients, C_L, at V/c=0.65, for 3R family

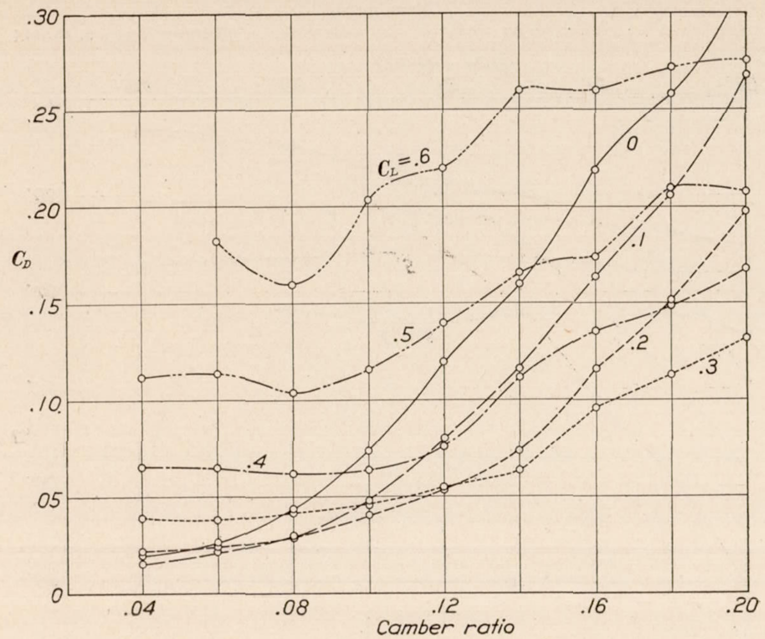

FIGURE 18.—Drag coefficient, C_D vs. camber ratio for various lift coefficients, C_L, at V/c=0.80, for 3R family

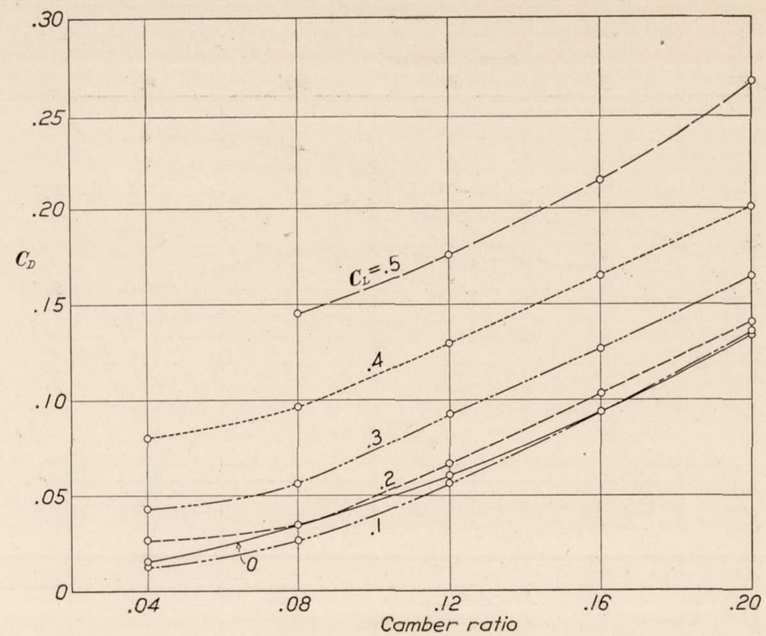

FIGURE 19.—Drag coefficient, C_D vs. camber ratio for various lift coefficients, C_L, at V/c=0.95 for 3R family

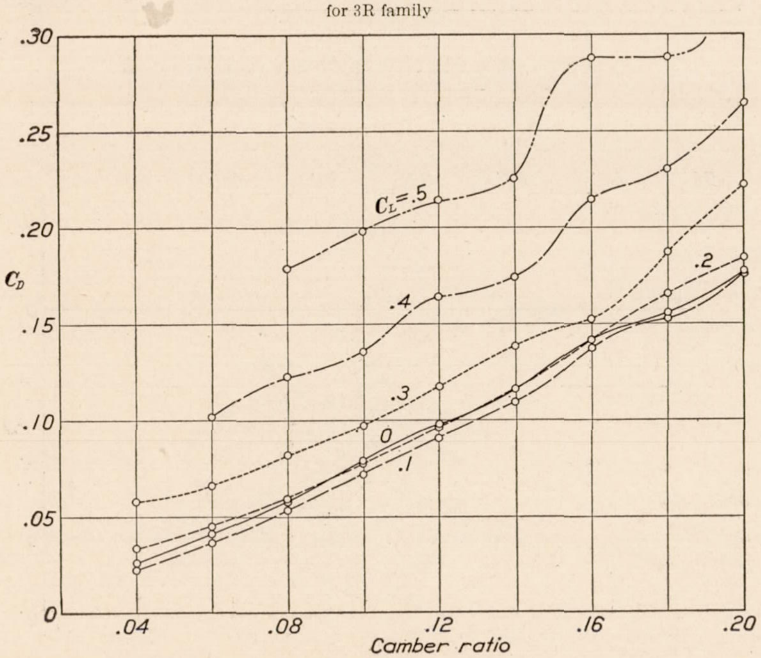

FIGURE 20.—Drag coefficient, C_D vs. camber ratio for various lift coefficients, C_L, at V/c=1.08, for 3R family

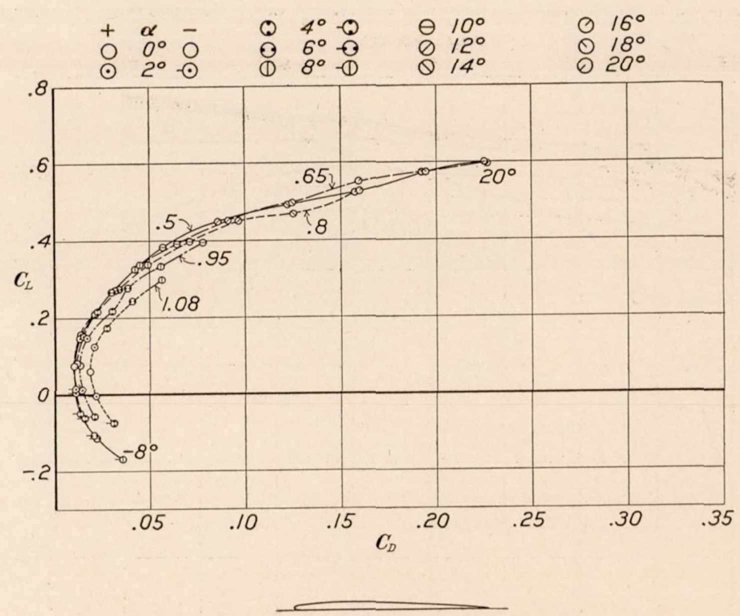

FIGURE 21.—Polar diagrams for airfoil C4 for five values of V/c

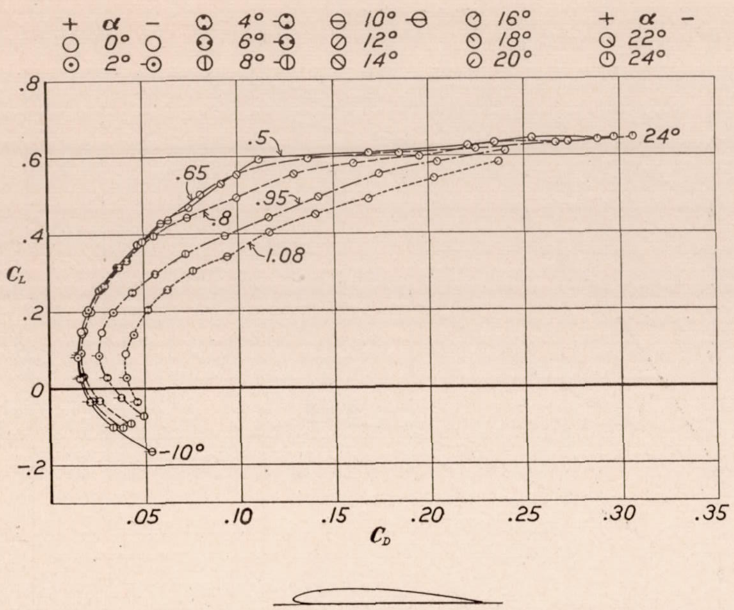

FIGURE 22.—Polar diagrams for airfoil C8 for five values of V/c

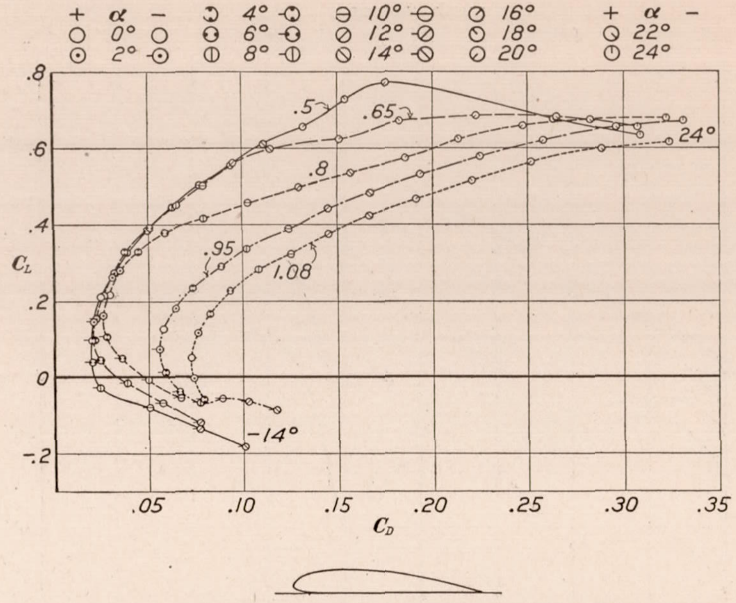

FIGURE 23.—Polar diagrams for airfoil C12 for five values of V/c

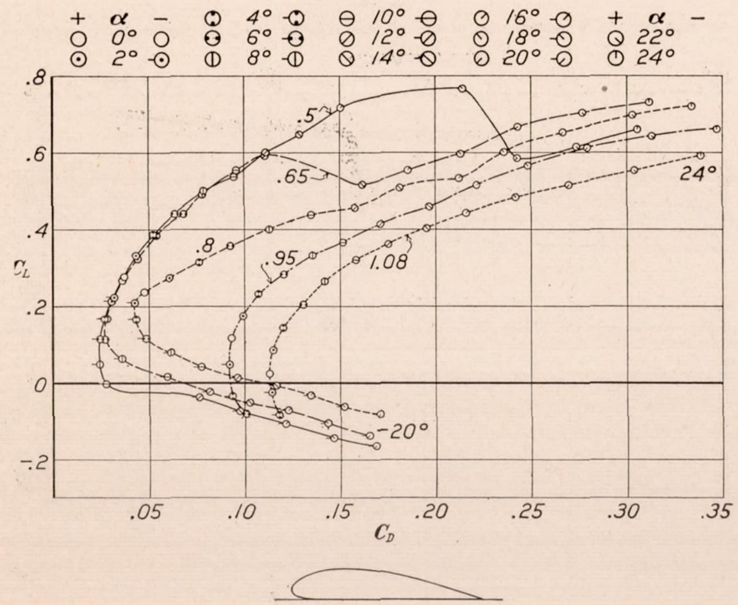

FIGURE 24.—Polar diagrams for airfoil C16 for five values of V/c

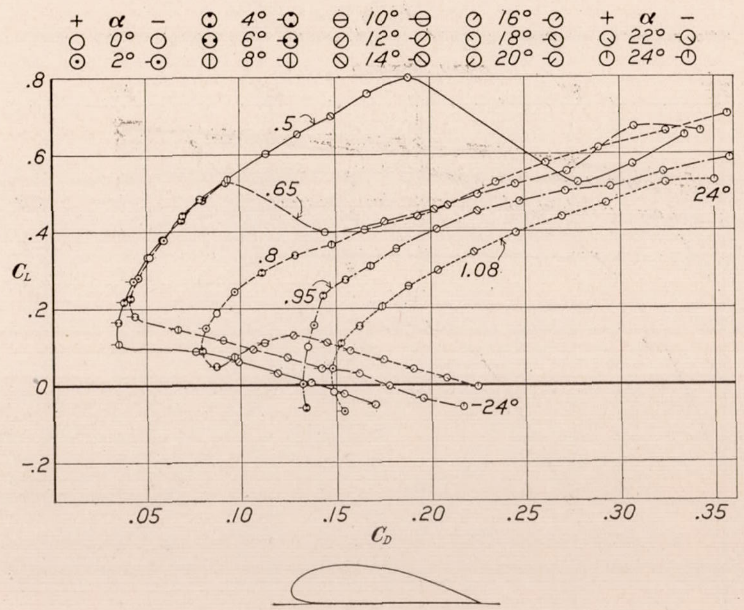

FIGURE 25.—Polar diagrams for airfoil C20 for five values of V/c

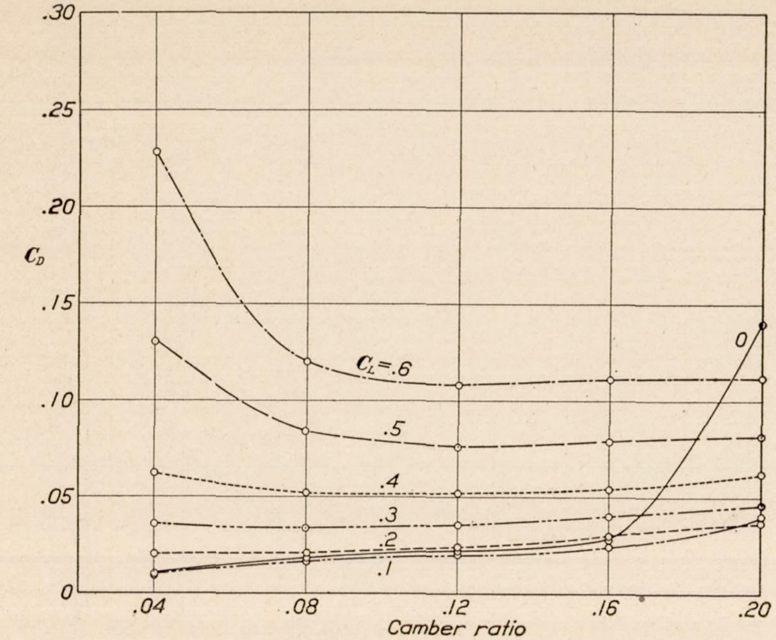

FIGURE 26.—Drag coefficient, C_D vs. camber ratio for various lift coefficients, C_L, at $V/c=0.50$, for C family

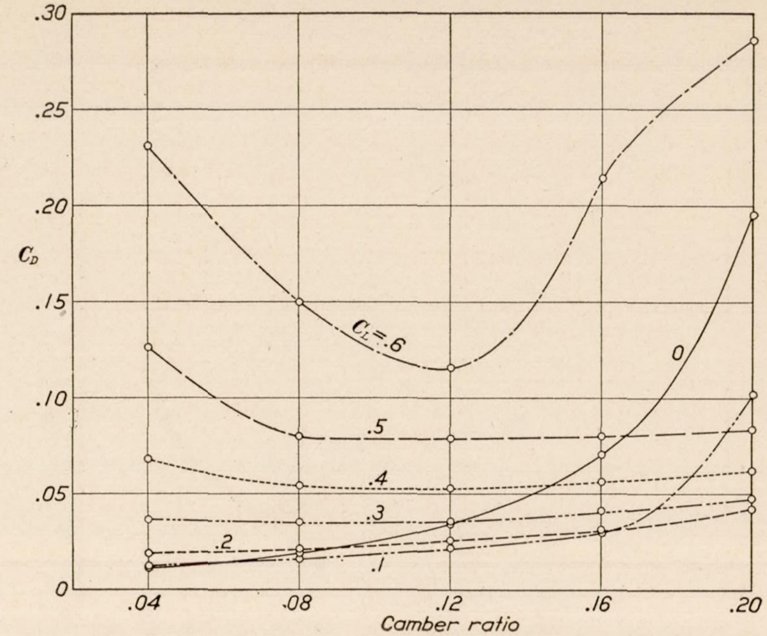

FIGURE 27.—Drag coefficient, C_D vs. camber ratio for various lift coefficients, C_L, at $V/c=0.65$, for C family

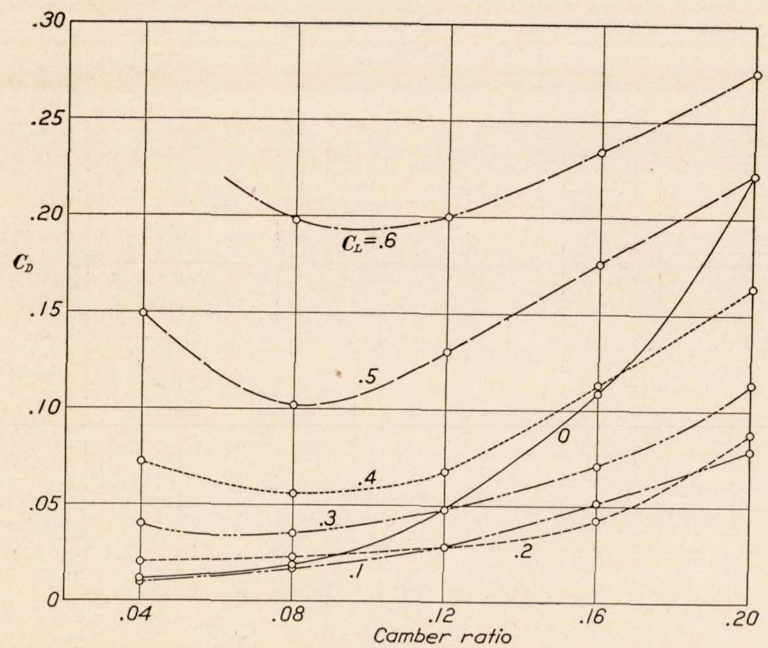

FIGURE 28.—Drag coefficient, C_D vs. camber ratio for various lift coefficients, C_L, at $V/c=0.80$, for C family

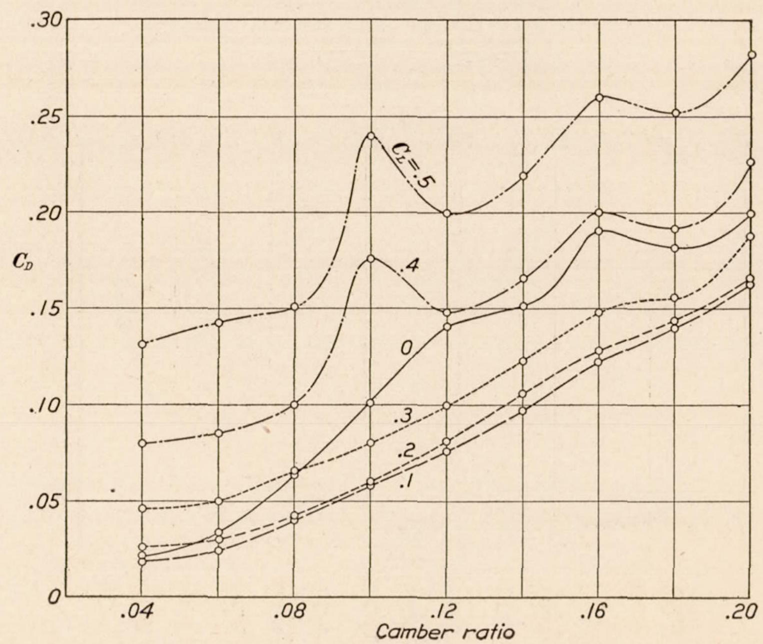

FIGURE 29.—Drag coefficient, C_D vs. camber ratio for various lift coefficients C_L, at $V/c=0.95$, for C family

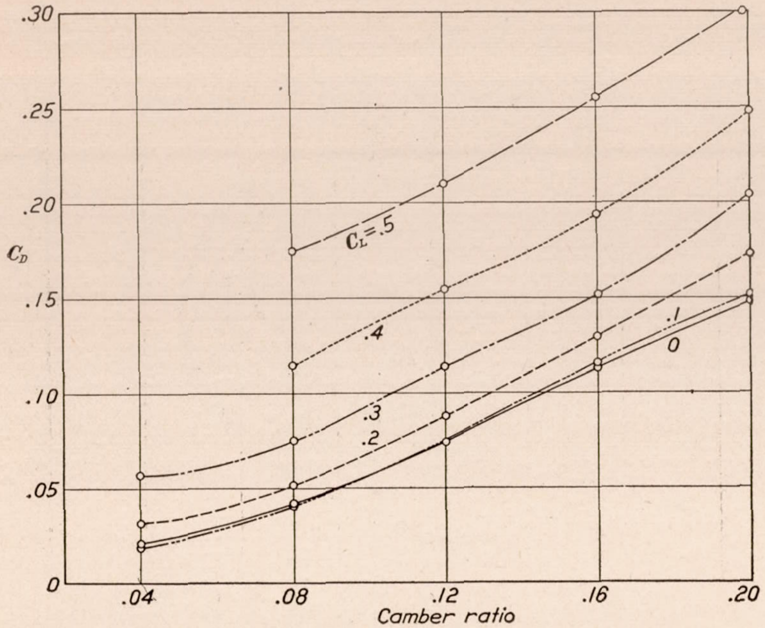

FIGURE 30.—Drag coefficient, C_D vs. camber ratio for various lift coefficients, C_L, at V/c=1.08, for C family

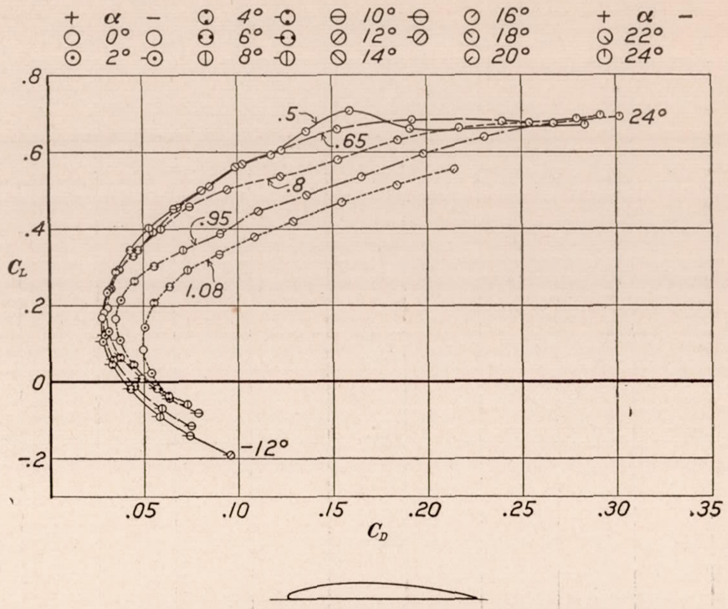

FIGURE 31.—Polar diagrams for airfoil 4R8 for five values of V/c

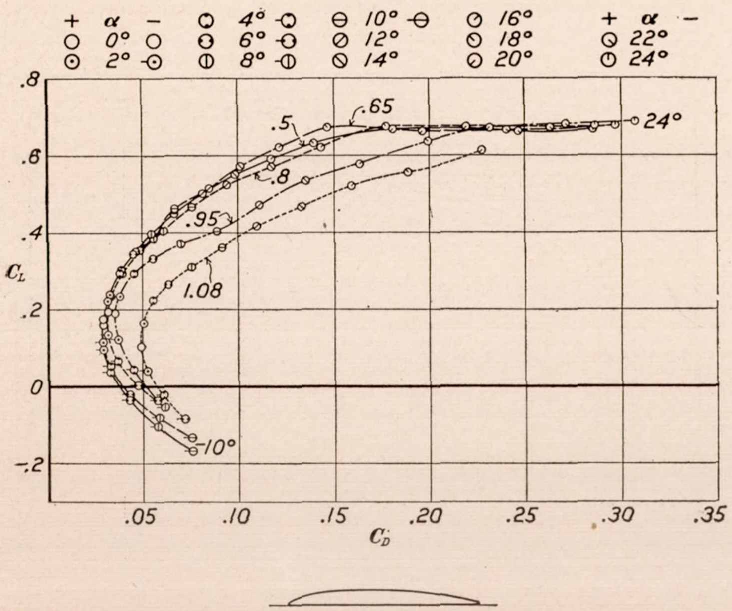

FIGURE 32.—Polar diagrams for airfoil 5R8 for five values of V/c

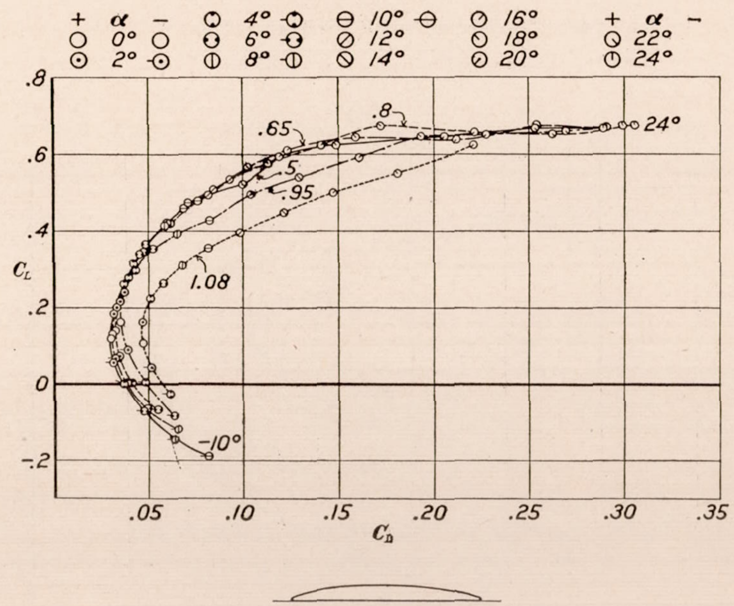

FIGURE 33.—Polar diagrams for airfoil 6R8 for five values of V/c

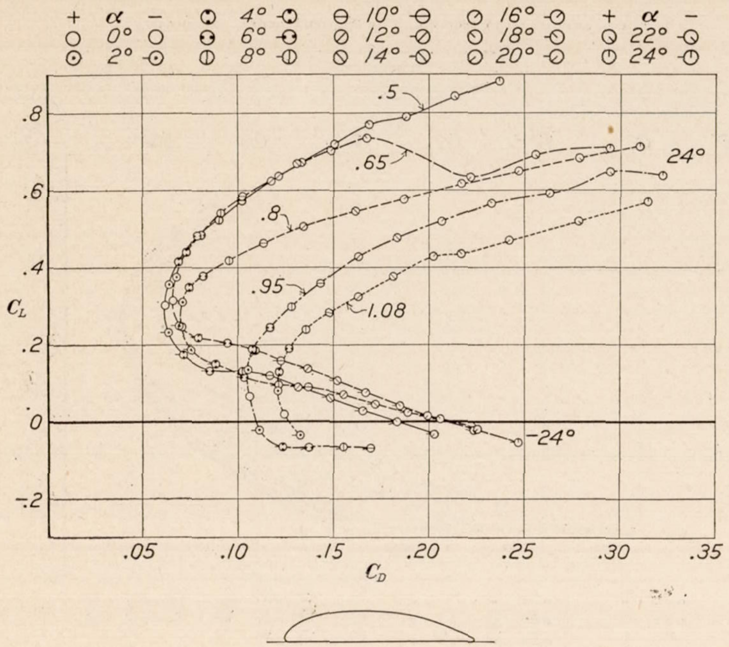

FIGURE 34.—Polar diagrams for airfoil 4R16 for five values of V/c

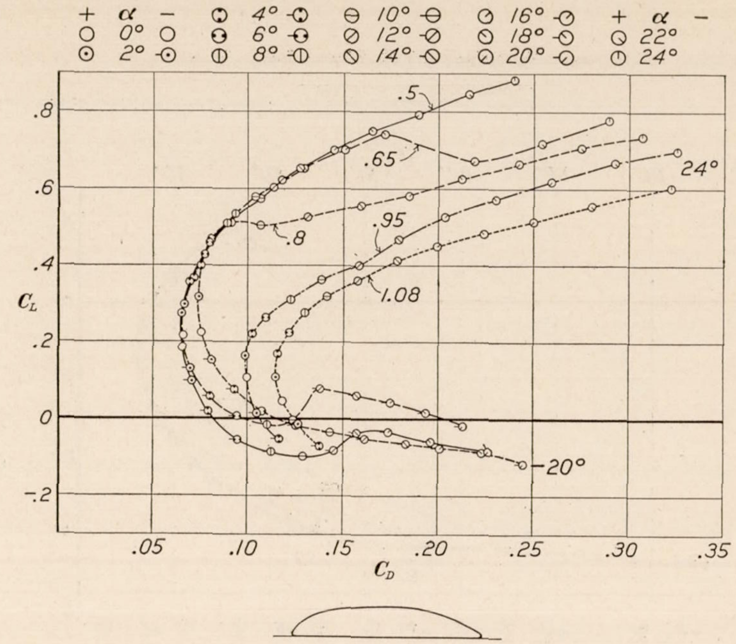

FIGURE 35.—Polar diagrams for airfoil 5R16 for five values of V/c

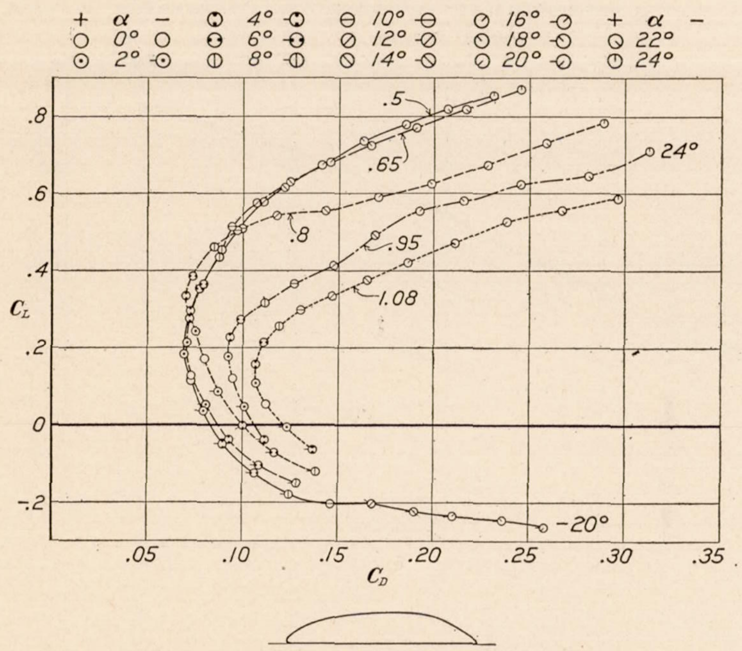

FIGURE 36.—Polar diagrams for airfoil 6R16 for five values of V/c

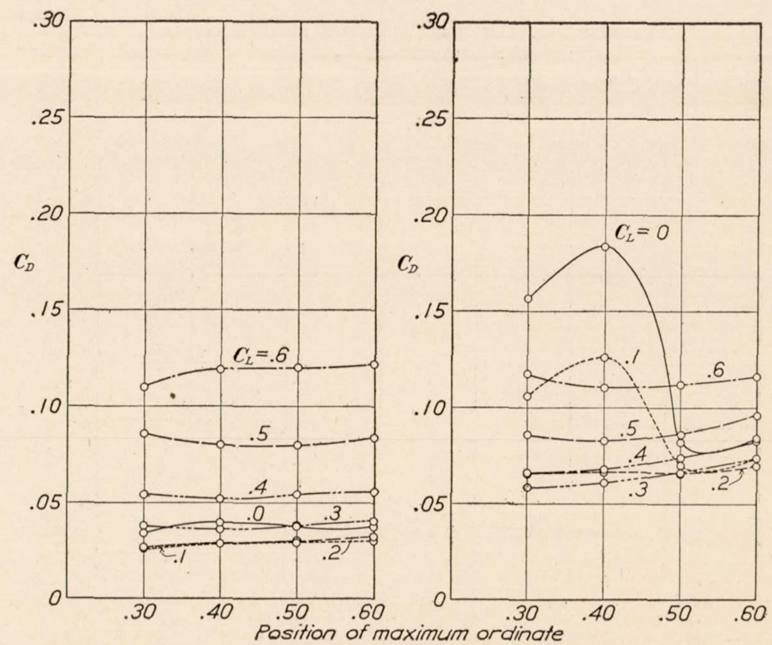

FIGURE 37.—Drag coefficient, C_D vs. position of maximum ordinate for various lift coefficients, C_L, at V/c=0.50 for R family

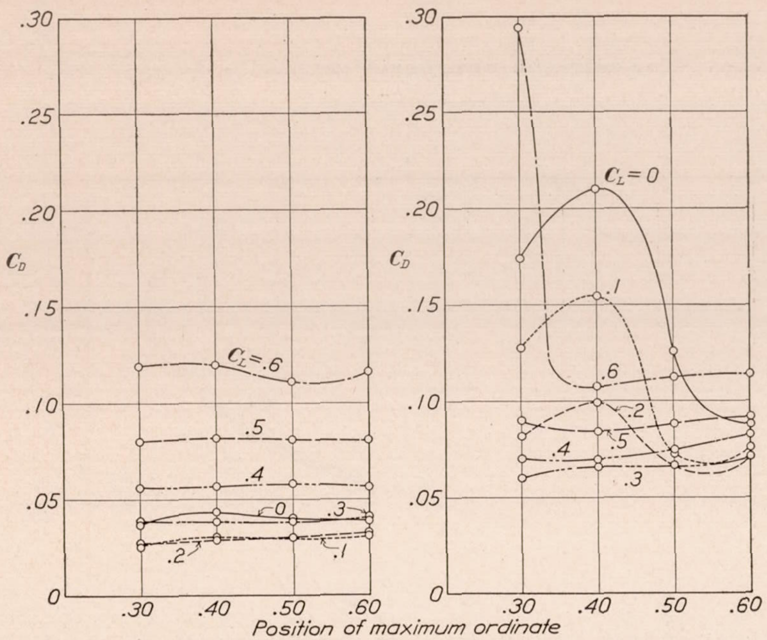

FIGURE 38.—Drag coefficient, C_D vs. position of maximum ordinate for various lift coefficients, C_L, at V/c=0.65 for R family

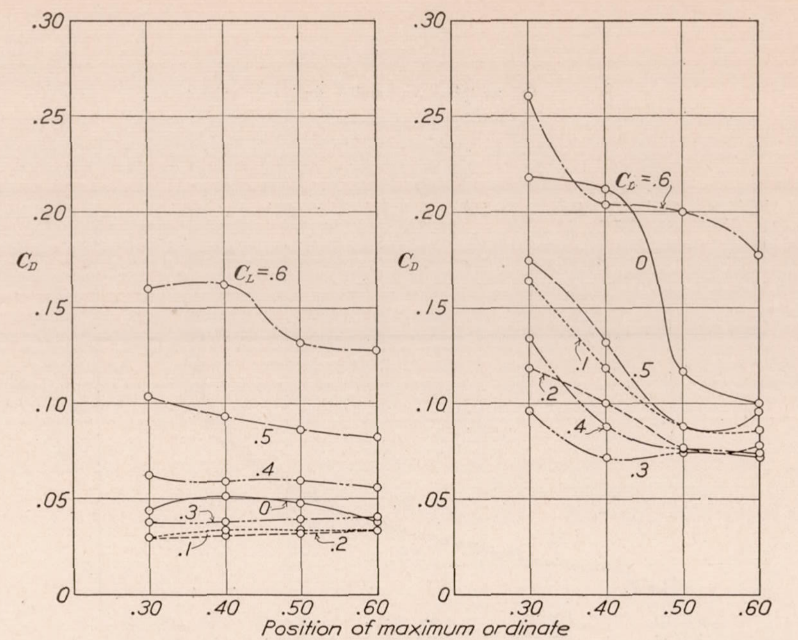

FIGURE 39.—Drag coefficient, C_D vs. position of maximum ordinate for various lift coefficients, C_L, at V/c=0. 80 for R family

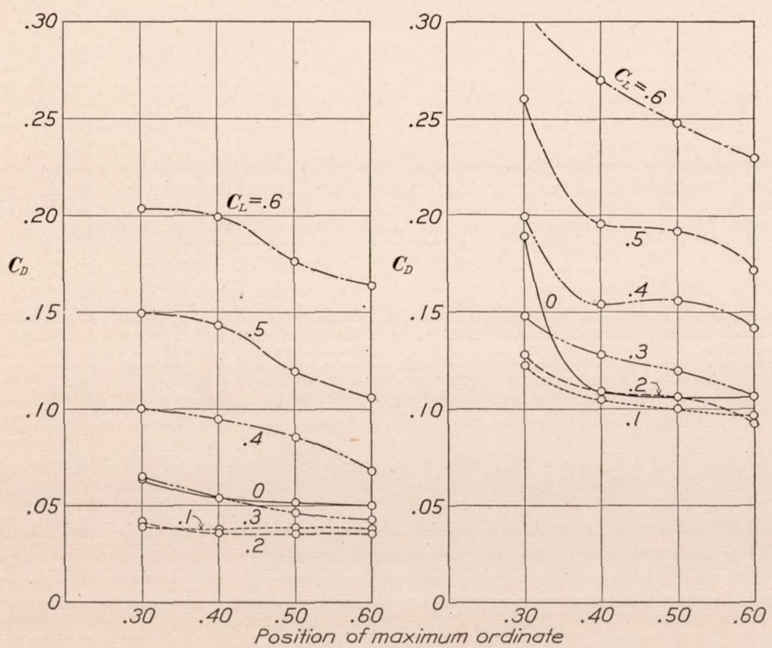

FIGURE 40.—Drag coefficient, C_D vs. position of maximum ordinate for various lift coefficients, C_L, at V/c=0.95 for R family

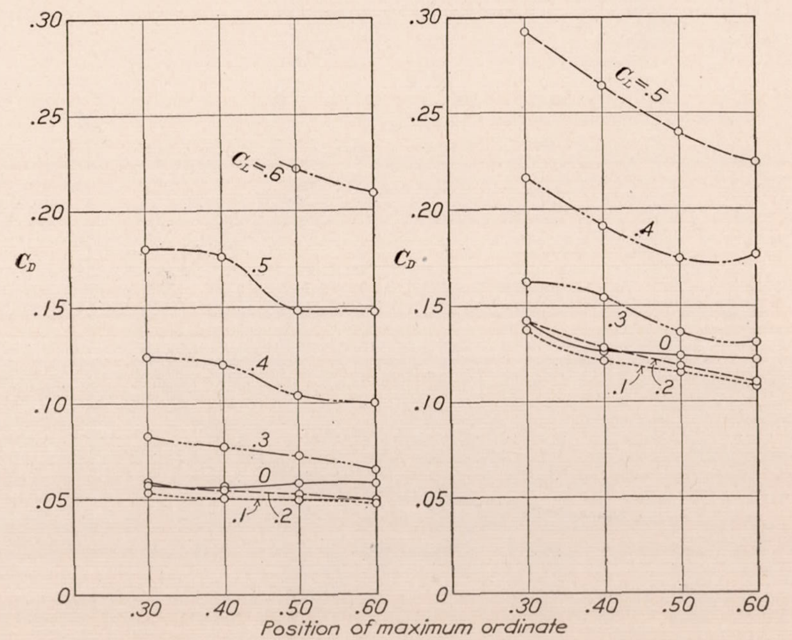

FIGURE 41.—Drag coefficient, C_D vs. position of maximum ordinate for various lift coefficients, C_L, at V/c=1.08 for R family

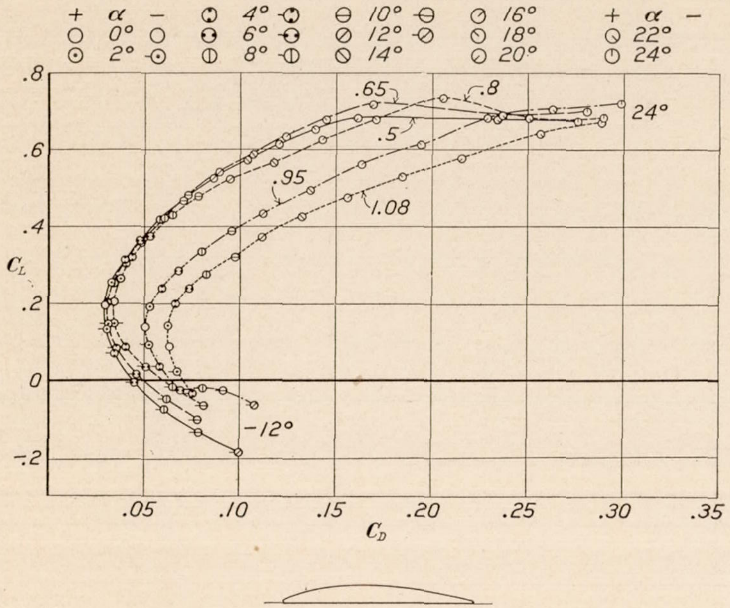

FIGURE 42.—Polar diagram for Reed airfoil for five values of V/c

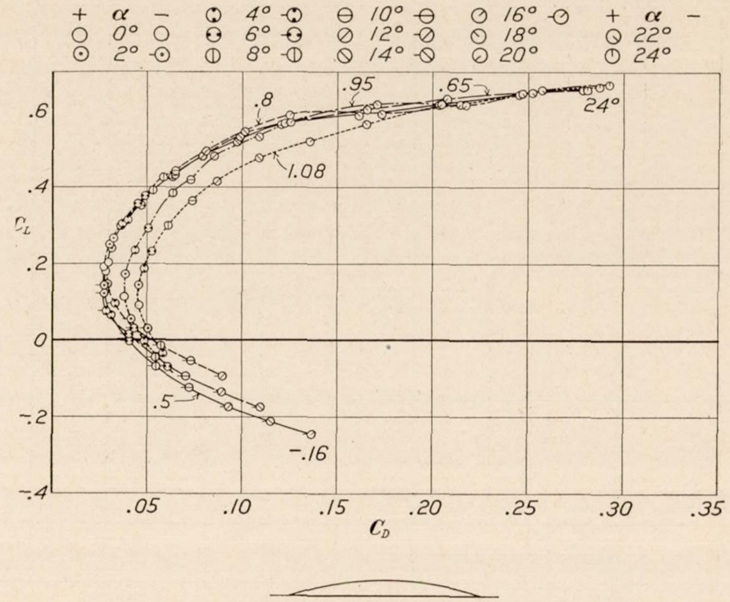

FIGURE 43.—Polar diagram for circular arc airfoil for five values of V/c

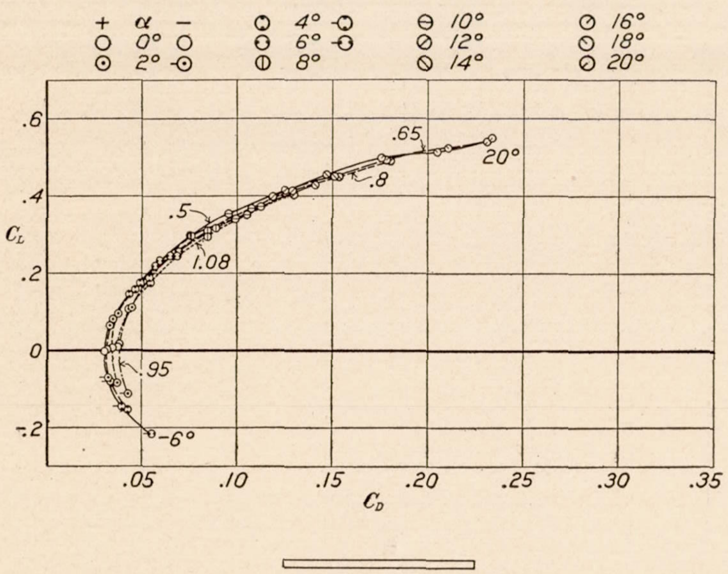

FIGURE 44.—Polar diagram for flat plate for five values of V/c

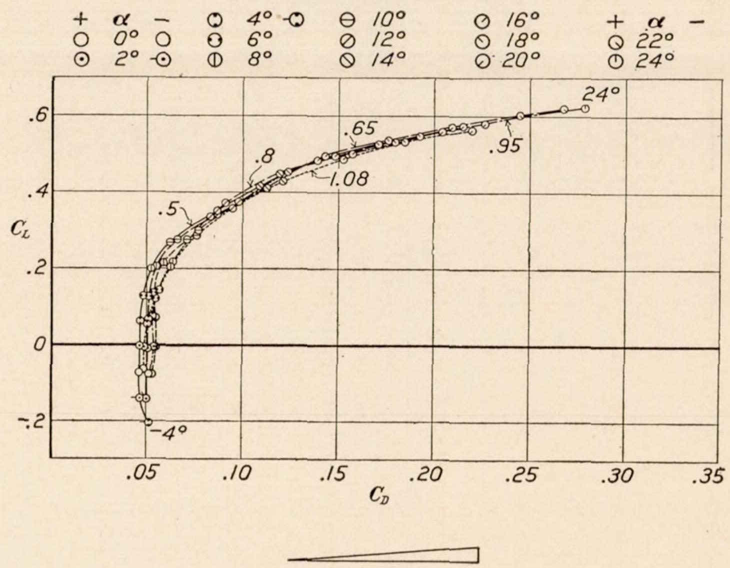

FIGURE 45.—Polar diagram for wedge for five values of V/c

The alignment of the air stream was checked as in our earlier work by moving the balance to the opposite side of the stream so that the lift direction was reversed with respect to the air stream. Good agreement was obtained between the normal runs and the runs with airfoil reversed.

We may say, therefore, that it is possible to repeat measurements under given conditions with satisfactory precision, but the characteristics of flow over thick sections are such that small changes in the end conditions at the edge of the jet produce noticeable systematic effects. The speed effect is, however, much greater so that the position effect does not at all obscure the main changes. Moreover, the position effect is of the same general nature for all airfoils so that the results from a comparative standpoint are believed to be reliable.

COMPARISON OF FORCE MEASUREMENTS WITH PRESSURE DISTRIBUTION MEASUREMENTS

Airfoil sections 3R10, 3R12, 3R14, 3R16, 3R18, and 3R20 were used in the pressure distribution measurements described in N. A. C. A. Technical Report No. 255 (Reference 3). Consequently, a comparison may be made between the integration of the pressure distribution at the central section and the average force on the whole airfoil. No general relation applicable to all airfoil sections and to all speeds appears to exist, and a detailed comparison of each section and speed does not seem advisable. In the ideal elliptical distribution of lift, the lift coefficient for the central section is greater than the average lift cofficient for the whole airfoil, in the ratio of 1 to $\pi/4$, and the induced drag is distributed in the same manner. Now even at low speeds the distribution of lift over an airfoil of rectangular plan form is not exactly elliptical but under conditions of smooth flow the lift at the central section is greater than the lift for the whole section. This same qualitative relation is found to hold in the high-speed tests where the flow is smooth; that is, for thin sections, small angles of attack, and at the lower speeds.

At the higher speeds the situation is quite different, for the breaking away of the flow from the surface occurs first at the center of the airfoil and consequently the lift is lowest at the central section and the drag is greatest. This fact was not adequately appreciated in N. A. C. A. Technical Report No. 255 (Reference 3) and the conclusions regarding the influence of Reynolds Number on the drag coefficient are not supported by the force measurements. The drag coefficient in the pressure distribution measurements was high as compared with the Lynn measurements, not because of the smaller model but because the inefficient type of flow occurs first at the center where the pressure distribution measurements were made.

As a result of this fact the pressure distribution measurements show the decrease in lift and increase in drag occurring at a somewhat lower speed and the differences in the curves for $V/c=0.5$ and $V/c=1.08$ are somewhat greater than for the force measurements. The force measurements average the inefficient flow at the center with the more efficient flow near the ends.

It should be emphasized here that the flow at high speeds is of the same general appearance as burbling flow at low speeds and just as no theory has been worked out for burbling flow, so no theory is available for the high-speed type of flow. Corrections for aspect ratio can not be computed and the estimation of interference between blade elements of propellers can not be based on the theory of induced drag. We hope to carry out later some experiments on the effects of aspect ratio.

For the present no method is known of using the coefficients of this report quantitatively for full-scale propeller computations due largely to our ignorance of methods of treating burbling flow. The curves are, however, self-consistent and are believed trustworthy for the comparison of airfoil sections as to their efficiency at high speeds.

COMPARISON OF R. A. F. AND CLARK Y FAMILIES.—An inspection of the table and curves shows that the Clark Y sections are more efficient than the R. A. F. sections (comparing sections of equal thickness) under all conditions except for very thin sections at high lift coefficients (Figs. 6, 8, 21, and 22). The Clark Y thin sections do not attain as high a maximum lift as the R. A. F. thin sections so that the polar curves cross at high lift coefficients, and under these conditions the R. A. F. sections give lower drag coefficients.

The ratio of the efficiencies of Clark Y and R. A. F. sections varies greatly with the thickness of section and with the speed. To illustrate the diversity of relationship of the two families, a detailed study is given of the variations of the minimum drag coefficient. Values taken from the tabulated values are summarized in the following table and the ratios for the two families are shown in the last column.

Thickness ratio	V/c	Minimum drag coefficient		Ratio $\frac{\text{R. A. F.}}{\text{Clark}}$
		R. A. F. family	Clark Y family	
0.04	0.50	0.016	0.010	1.60
	.65	.016	.011	1.45
	.80	.016	.011	1.45
	.95	.018	.013	1.38
	1.08	.022	.019	1.16
.08	.50	.025	.016	1 56
	.65	.026	.016	1 62
	.80	.029	.017	1.71
	.95	.039	.027	1.45
	1.08	.053	.040	1.32
.12	.50	.045	.020	2.25
	.65	.046	.021	2.19
	.80	.052	.026	2.00
	.95	.076	.056	1.36
	1.08	.090	.073	1.23
.16	.50	.059	.025	2.36
	.65	.068	.028	2.43
	.80	.073	.043	1.70
	.95	.123	.092	1.34
	1.08	.138	.112	1.23
.20	.50	.076	.035	2.17
	.65	.078	.042	1.86
	.80	.115	.079	1.46
	.95	.163	.131	1.24
	1.08	.175	.148	1.18

It will be noted that at the two low speeds, the ratio is approximately 1.6 for thickness ratios of 0.04 and 0.08, while for thickness ratios of 0.12, 0.16, and 0.20 the ratio is over 2. A curve of the ratio plotted against thickness-ratio is seen to rise rapidly between 0.08 and 0.12, reach a maximum near 0.16, and then fall off a little. In other words, the ratio of the minimum drag of the R. A. F. sections to that of the Clark Y sections is much greater for thick sections than for thin sections and a rapid increase occurs between a thickness-ratio of 0.08 and 0.12 when the speed is below 0.65 the speed of sound. The single value obtainable from ordinary wind tunnel tests N. A. C. A. Technical Reports Nos. 233 and 259 (References 5 and 4, respectively) at the same Reynolds Number is 2.3 for a thickness-ratio of approximately 0.12 and is in good agreement with the above values.

At the higher speeds, on the other hand, the ratio is nearly independent of thickness ratio and is much lower, namely, about 1.25. Hence the relative advantage of Clark Y sections is less at the higher speeds.

The effect of speed may be shown most readily by means of a separate table.

Thickness ratio	Ratio of minimum drag at $V/c=1.08$ to $V/c=0.50$	
	R. A. F. family	Clark Y family
0. 04	1. 38	1. 90
. 08	2. 12	2. 56
. 12	2. 00	3. 65
. 16	2. 34	4. 48
. 20	2. 30	4. 23

The increase in the minimum drag coefficient with speed is much greater for the Clark Y family than for the R. A. F. family. Also, the increase with speed reaches a nearly constant value in the R. A. F. family for a thickness ratio of 0.08, whereas in the Clark Y family the maximum is not reached until a thickness ratio of 0.16 is attained.

Propeller sections are practically never run at the low lift coefficients corresponding to minimum drag, the lift coefficient usually being greater than 0.4. The above comparison can not therefore be considered as representing the relative merits of the two families for use in the design of propellers. So long as the thickness of the section is one-tenth the chord or greater, the Clark Y family shows an advantage in all cases. For thinner sections the two families give approximately the same results. Our experiments on thin sections do not cover the full range because at high angles and speeds the thin airfoils were deformed by the air-stream.

The curves of Figures 15 to 20 and 26 to 30 give an opportunity for comparison under a great variety of conditions. Figure 15 is plotted from the data given by E. N. Jacobs in N. A. C. A. Technical Report No. 259. (Reference 4.) It shows that for low and moderate lift coefficients thin sections are the most efficient. Thick sections give greatly increased drag for very low lift coefficients due to the fact that the angle of attack is negative and a burbling type of flow results. Figure 16 shows results for a speed of one-half the speed of sound. The curves are similar in nature to the low-speed tests except that the lift coefficients obtained are much lower due to the small aspect ratio. The increased drag for thick sections at low lift coefficients also covers a wider field of thickness ratio and lift coefficient. This region spreads as the speed is increased (Figs. 17 and 18) until for a speed of 0.95 the speed of sound (Fig. 19), thin sections are best for all lift coefficients. For a speed of 1.08 times the speed of sound (Fig. 20) an approximately linear variation of the drag (for a given lift) with thickness ratio is found.

Figure 26 for the Clark Y family at a speed of one-half the speed of sound shows that over a wide range of thickness ratio the drag for a given lift is roughly constant. However, the same changes occur and for $V/c=0.8$ (Fig. 28) we have already a suggestion of the character finally developed in Figures 29 and 30 for the higher speeds. Comparison of Figures 20 and 30 show the greater slope and hence the greater speed effect for the Clark Y family.

These examples serve to illustrate the complexity of the relationships found. Perhaps the best general statement that can be made is that when the flow is no longer smooth, all sections are brought more nearly to the same level irrespective of their efficiencies when the flow is smooth. The efficient sections therefore suffer most.

When the thickness is 0.10 the chord or greater, the use of the Clark Y type of section at high speeds is, however, most desirable on account of a 25 per cent decrease in minimum drag. The great advantage of using as thin a section as possible is also clearly apparent.

The present experiments do not indicate any advantage for the Clark Y family when sections thinner than 0.10 the chord are used in modern thin blade metal propellers.

EFFECT OF POSITION OF MAXIMUM ORDINATE

Figures 37 to 41, inclusive, show the effect of the position of the maximum ordinate, which is of less magnitude than the effect of thickness or of speed. At a speed of 0.5 the speed of sound the 30 per cent position of the maximum ordinate is best except for the thick sections at very low lift coefficients. As the speed increases it is advantageous to move the maximum ordinate further back, especially in the case of the thick sections. As the effect is relatively small for thin sections and at low speeds it is recommended that no change be made except for sections of thickness ratio greater than 0.12 for use at speeds greater than 0.9 the speed of sound.

Conclusions.—The more important general conclusions are as follows:

1. The Clark Y family is more efficient than the R. A. F. family (sections of equal thickness being compared) when the thickness is greater than 0.10 the chord. The Clark Y thin sections do not attain as high a maximum lift as the R. A. F. thin sections, so that the polar curves cross at high lift coefficients and the R. A. F. sections under these conditions give less drag.

2. At high speeds, the maximum ordinate on thick sections should be moved back to secure the best results. The minimum drag is often increased but the drag at high lift coefficients is decreased and at very high speeds the minimum drag is also decreased.

3. In most cases the flow leaves the rear part of the upper surface at all positive angles of attack at speeds above approximately 0.8 the speed of sound.

4. The thinner sections maintain their lift coefficients very well to the highest speeds, but the thicker sections show a marked decrease in lift coefficient. The total lift actually decreases as the speed increases over a certain range.

5. All sections show a marked increase in drag coefficient with increasing speed, the rate of increase rising rather abruptly at a speed well below the speed of sound. At large angles of attack the drag coefficient reaches a maximum approximately at the speed of sound.

6. Airfoil sections are more efficient at high speeds than a flat plate or wedge. A cylindrical segment in the single test made was found to be somewhat more efficient than the airfoil sections.

7. Aspect ratio effects are large. A theory of these effects is available only for the lower speeds where the type of flow is relatively smooth. In this case the theoretical minimum induced drag is the same as for aspect ratio 2. Since, however, no theoretical laws for aspect-ratio effects have been developed for the types of flow observed at high speeds, the measurements in the 2-inch air stream must be considered as qualitative in character until the correction for aspect ratio is known. (References 1 and 6.)

Bureau of Standards,
Washington, D. C., *August 7, 1928.*

REFERENCES

1. Briggs, L. J., Hull, G. F., and Dryden, H. L.: Aerodynamic Characteristics of Airfoils at High Speeds. N. A. C. A. Technical Report No. 207. (1925.)
2. Caldwell, F. W., and Fales, E. N.: Wind Studies in Aerodynamic Phenomena at High Speed. Part I. Model Wind Tunnel Experiments. Part II. The McCook Field Wind Tunnel. Part III. Model Tests on Propeller Aerofoils. N. A. C. A. Technical Report No. 83. (1920.)
3. Briggs, L. J., and Dryden, H. L.: Pressure Distribution Over Airfoils at High Speeds. N. A. C. A. Technical Report No. 255. (1927.)
4. Jacobs, Eastman N.: Characteristics of Propeller Sections Tested in the Variable Density Wind Tunnel. N. A. C. A. Technical Report No. 259. (1927.)
5. Munk, Max M., and Miller, Elton W.: The Aerodynamic Characteristics of Seven Frequently Used Wing Sections at Full Reynolds Number. N. A. C. A. Technical Report No. 233. (1926.)
6. Kumbruch, H.: Zeitschrift für Flugtechnik und Motorluftschiffahrt, Vol. X, Nos. 9 and 10.

TABLE I.—ORDINATES OF AIRFOILS

RAF Family

ORDINATES OF UPPER SURFACE

Distance from nose	3R4	3R6	3R8	3R10	3R12	3R14	3R16	3R18	3R20
0.025	0.016	0.024	0.032	0.041	0.049	0.057	0.065	0.073	0.082
.050	.024	.035	.047	.059	.070	.082	.094	.106	.118
.100	.032	.047	.063	.079	.094	.110	.126	.142	.158
.200	.038	.057	.076	.095	.114	.133	.152	.171	.190
.300	.040	.060	.080	.100	.120	.140	.160	.180	.200
.400	.040	.059	.079	.099	.118	.138	.158	.178	.198
.500	.038	.057	.076	.095	.114	.133	.152	.171	.190
.600	.035	.052	.069	.087	.104	.121	.139	.156	.174
.700	.030	.044	.059	.094	.088	.103	.118	.133	.148
.800	.022	.033	.044	.056	.067	.078	.089	.100	.112
.900	.014	.021	.028	.035	.042	.049	.056	.063	.070

NOTE.—Lower surface is plane.

Distance from nose	4R8	5R8	6R8	4R16	5R16	6R16
0.050	0.042	0.037	0.032	0.084	0.075	0.065
.100	.057	.052	.047	.113	.104	.094
.200	.070	.067	.063	.141	.134	.126
.300	.078	.074	.071	.156	.149	.142
.400	.080	.078	.076	.160	.157	.152
.500	.079	.080	.079	.158	.160	.158
.600	.074	.078	.080	.148	.156	.160
.700	.065	.071	.077	.130	.142	.154
.800	.050	.056	.064	.100	.112	.129
.900	.030	.039	.040	.061	.079	.081

NOTE.—Lower surface is plane.

Clark Y Family

ORDINATES OF UPPER AND LOWER SURFACES

Distance from nose	C 4		C 8		C 12		C 16		C 20	
	Upper	Lower	Upper	Lower	Upper	Lower	Upper	Lower	Upper	Lower
0.000	0.012	0.012	0.024	0.024	0.037	0.037	0.048	0.048	0.061	0.061
.025	.022	.005	.044	.010	.066	.015	.088	.020	.110	.025
.050	.027	.003	.054	.006	.080	.009	.107	.012	.134	.016
.075	.031	.002	.061	.004	.092	.006	.122	.008	.153	.010
.100	.033	.001	.065	.003	.098	.004	.131	.005	.164	.006
.150	.036	.000	.073	.001	.109	.001	.146	.002	.182	.003
.200	.039	.000	.078	.000	.116	.000	.155	.000	.193	.000
.300	.040	.000	.080	.000	.120	.000	.160	.000	.200	.000
.400	.039	.000	.078	.000	.117	.000	.156	.000	.195	.000
.500	.036	.000	.072	.000	.108	.000	.144	.000	.180	.000
.600	.031	.000	.062	.000	.094	.000	.125	.000	.156	.000
.700	.025	.000	.050	.000	.075	.000	.100	.000	.126	.000
.800	.018	.000	.036	.000	.053	.000	.071	.000	.089	.000
.900	.010	.000	.019	.000	.029	.000	.037	.000	.048	.000

Reed section	
Distance from nose	Ordinate of upper surface
0. 100	0. 056
. 200	. 080
. 300	. 094
. 400	. 094
. 500	. 091
. 600	. 084
. 700	. 074
. 800	. 058
. 900	. 039

NOTE.—Lower surface plane.

Flat plate is 0.04 inch by 1 inch.
Wedge is 0.08 inch at base by 1 inch.
Circular arc airfoil has a plane lower surface and a maximum ordinate of 0.08 inch.
The chord is 1 inch in all cases.

TABLE II.—LIFT AND DRAG COEFFICIENTS OF AIRFOILS AT VARYING ANGLES OF ATTACK FOR DIFFERENT VALUES OF V/c

AIRFOIL 3R4

LIFT COEFFICIENTS C_L

V/c	Angle of attack											
	−4	−2	0	2	4	6	8	10	12	14	16	20
0. 50	−0. 043	0. 017	0. 085	0. 154	0. 214	0. 273	0. 340	0. 394	0. 461	0. 506	0. 558	0. 604
. 65	−. 047	. 017	. 086	. 156	. 217	. 271	. 326	. 394	. 462	. 508	. 558	. 610
. 80	−. 052	. 017	. 087	. 151	. 217	. 266	. 339	. 402	. 458	. 508	. 544	-------
. 95	−. 056	. 010	. 081	. 151	. 218	. 277	. 336	. 392	. 451	. 506	-------	-------
1. 08	−. 067	. 003	. 068	. 130	. 188	. 245	. 296	-------	-------	-------	-------	-------

DRAG COEFFICIENTS C_D

V/c	−4	−2	0	2	4	6	8	10	12	14	16	20
0. 50	0. 023	0. 017	0. 016	0. 018	0. 022	0. 030	0. 041	0. 054	0. 070	0. 092	0. 136	0. 219
. 65	. 024	. 018	. 016	. 018	. 024	. 030	. 042	. 056	. 075	. 104	. 140	. 220
. 80	. 026	. 019	. 016	. 019	. 025	. 033	. 047	. 067	. 091	. 117	. 149	-------
. 95	. 029	. 021	. 018	. 021	. 029	. 041	. 056	. 077	. 103	. 133	-------	-------
1. 08	. 037	. 026	. 022	. 024	. 031	. 043	. 057	-------	-------	-------	-------	-------

AIRFOIL 3R6

LIFT COEFFICIENTS C_L

V/c	Angle of attack											
	−4	−2	0	2	4	6	8	10	12	14	16	20
0. 50	−0. 033	0. 033	0. 104	0. 174	0. 229	0. 281	0. 344	0. 401	0. 458	0. 510	0. 575	0. 649
. 65	−. 018	. 044	. 112	. 170	. 229	. 287	. 335	. 397	. 459	. 510	. 572	. 635
. 80	−. 017	. 054	. 116	. 172	. 225	. 294	. 351	. 408	. 464	. 503	. 555	. 631
. 95	. 007	. 060	. 119	. 179	. 234	. 286	. 335	. 389	. 436	. 480	. 532	-------
1. 08	−. 033	. 030	. 096	. 139	. 200	. 261	. 310	. 364	. 423	-------	-------	-------

DRAG COEFFICIENTS C_D

V/c	−4	−2	0	2	4	6	8	10	12	14	16	20
0. 50	0. 027	0. 021	0. 018	0. 020	0. 025	0. 032	0. 043	0. 055	0. 070	0. 088	0. 108	0. 190
. 65	. 028	. 021	. 020	. 021	. 026	. 034	. 044	. 058	. 074	. 094	. 121	. 195
. 80	. 029	. 023	. 021	. 023	. 029	. 037	. 051	. 068	. 090	. 115	. 144	. 210
. 95	. 033	. 027	. 025	. 027	. 035	. 047	. 062	. 081	. 104	. 128	. 157	-------
1. 08	. 045	. 039	. 037	. 039	. 045	. 056	. 071	. 088	. 111	-------	-------	-------

Airfoil 3R8

LIFT COEFFICIENTS C_L

V/c	Angle of attack											
	−4	−2	0	2	4	6	8	10	12	14	16	20
0.50	0.023	0.094	0.155	0.209	0.264	0.324	0.381	0.433	0.473	0.561	0.618	0.686
.65	.033	.099	.157	.216	.272	.328	.374	.452	.502	.563	.608	.672
.80	.045	.105	.165	.221	.276	.337	.394	.450	.495	.537	.597	.654
.95	.054	.103	.158	.211	.254	.293	.346	.398	.440	.490	.540	.638
1.08	−.039	.016	.086	.150	.219	.262	.293	.339	.369	.424	.466	.576

DRAG COEFFICIENTS C_D

0.50	0.031	0.026	0.025	0.027	0.033	0.042	0.051	0.064	0.079	0.098	0.117	0.178
.65	.032	.027	.026	.028	.035	.043	.053	.066	.082	.101	.122	.204
.80	.036	.030	.029	.032	.038	.048	.061	.079	.100	.128	.157	.224
.95	.045	.040	.039	.043	.051	.063	.079	.099	.120	.143	.171	.236
1.08	.063	.056	.053	.055	.062	.070	.081	.097	.114	.135	.159	.226

Airfoil 3R10

LIFT COEFFICIENTS C_L

V/c	Angle of attack											
	−4	−2	0	2	4	6	8	10	12	14	16	20
0.50	0.086	0.144	0.206	0.257	0.322	0.378	0.427	0.481	0.517	0.569	0.642	0.753
.65	.092	.150	.208	.265	.321	.358	.430	.487	.546	.586	.579	.656
.80	.099	.160	.205	.261	.321	.371	.414	.459	.502	.520	.552	.642
.95	.068	.115	.160	.213	.254	.301	.343	.393	.437	.472	.528	.618
1.08	−.017	.038	.103	.160	.218	.270	.310	.356	.396	.446	.493	.569

DRAG COEFFICIENTS C_D

0.50	0.040	0.036	0.035	0.037	0.043	0.051	0.062	0.074	0.089	0.108	0.126	0.172
.65	.043	.038	.036	.038	.044	.045	.063	.077	.093	.110	.153	.220
.80	.048	.042	.040	.043	.049	.057	.072	.093	.116	.144	.174	.232
.95	.062	.058	.058	.061	.068	.080	.094	.112	.135	.160	.186	.248
1.08	.082	.075	.072	.074	.080	.089	.100	.116	.135	.158	.184	.241

Airfoil 3R12

LIFT COEFFICIENTS C_L

V/c	Angle of attack											
	−4	−2	0	2	4	6	8	10	12	14	16	20
0.50	0.113	0.176	0.240	0.292	0.340	0.382	0.445	0.499	0.558	0.597	0.656	0.750
.65	.129	.179	.237	.287	.349	.385	.456	.499	.554	.591	.593	.642
.80	.140	.188	.234	.296	.339	.381	.419	.453	.490	.523	.548	.642
.95	.063	.086	.145	.198	.243	.290	.343	.365	.407	.452	.496	.579
1.08	−.025	.027	.081	.136	.202	.247	.297	.331	.369	.414	.471	.538

DRAG COEFFICIENTS C_D

0.50	0.049	0.045	0.045	0.047	0.052	0.060	0.071	0.083	0.098	0.115	0.133	0.177
.65	.054	.048	.046	.047	.053	.061	.071	.084	.099	.118	.162	.233
.80	.064	.054	.052	.053	.059	.069	.086	.108	.131	.159	.185	.247
.95	.083	.077	.076	.081	.088	.097	.112	.128	.150	.174	.197	.255
1.08	.103	.094	.090	.090	.095	.103	.116	.131	.150	.170	.194	.247

Airfoil 3R14

LIFT COEFFICIENTS C_L

V/c	Angle of attack											
	−4	−2	0	2	4	6	8	10	12	14	16	20
0. 50	0. 142	0. 204	0. 266	0. 315	0. 360	0. 412	0. 468	0. 521	0. 547	0. 616	0. 680	0. 775
. 65	. 160	. 208	. 261	. 313	. 360	. 426	. 470	. 523	. 572	. 472	. 505	. 604
. 80	. 190	. 229	. 278	. 316	. 347	. 365	. 387	. 434	. 473	. 506	. 524	. 596
. 95	. 026	. 014	. 124	. 176	. 221	. 263	. 318	. 365	. 394	. 454	. 493	. 568
1. 08	−. 049	. 003	. 057	. 120	. 187	. 242	. 284	. 319	. 381	. 425	. 464	. 542

DRAG COEFFICIENTS C_D

V/c	−4	−2	0	2	4	6	8	10	12	14	16	20
0. 50	0. 059	0. 052	0. 050	0. 052	0. 056	0. 064	0. 075	0. 087	0. 098	0. 117	0. 136	0. 178
. 65	. 067	. 057	. 053	. 055	. 060	. 067	. 077	. 090	. 105	. 153	. 185	. 230
. 80	. 077	. 067	. 062	. 065	. 071	. 086	. 105	. 125	. 147	. 173	. 203	. 254
. 95	. 106	. 099	. 099	. 103	. 109	. 116	. 128	. 146	. 163	. 188	. 212	. 261
1. 08	. 122	. 115	. 111	. 109	. 114	. 121	. 132	. 147	. 165	. 185	. 207	. 262

Airfoil 3R16

LIFT COEFFICIENTS C_L

V/c	Angle of attack											
	−4	−2	0	2	4	6	8	10	12	14	16	20
0. 50	0. 181	0. 236	0. 298	0. 354	0. 399	0. 445	0. 490	0. 539	0. 592	0. 648	0. 716	0. 574
. 65	. 215	. 252	. 282	. 335	. 392	. 450	. 492	. 540	. 421	. 462	. 501	. 580
			. 308						. 445	. 483	. 552	. 635
. 80	. 231	. 259	. 247	. 259	. 307	. 344	. 386	. 430	. 461	. 496	. 528	. 614
. 95	. 032	. 048	. 086	. 167	. 223	. 267	. 311	. 359	. 380	. 421	. 457	. 549
1. 08	−. 079	−. 027	. 034	. 103	. 176	. 222	. 278	. 320	. 349	. 382	. 420	. 479

DRAG COEFFICIENTS C_D

V/c	−4	−2	0	2	4	6	8	10	12	14	16	20
0. 50	0. 069	0. 061	0. 059	0. 061	0. 066	0. 073	0. 084	0. 098	0. 115	0. 132	0. 151	0. 261
. 65	. 078	. 067	. 068	. 062	. 068	. 076	. 087	. 100	. 143	. 167	. 190	. 253
			. 060						. 162	. 190	. 216	
. 80	. 092	. 081	. 073	. 083	. 098	. 114	. 130	. 148	. 174	. 195	. 217	. 271
. 95	. 130	. 125	. 123	. 124	. 132	. 140	. 152	. 166	. 189	. 208	. 236	. 287
1. 08	. 150	. 144	. 138	. 138	. 140	. 145	. 155	. 170	. 185	. 205	. 225	. 272

Airfoil 3R18

LIFT COEFFICIENTS C_L

V/c	Angle of attack											
	−4	−2	0	2	4	6	8	10	12	14	16	20
0. 50	0. 224	0. 271	0. 340	0. 388	0. 433	0. 469	0. 505	0. 575	0. 620	0. 674	0. 735	0. 810
. 65	. 260	. 289	. 322	. 369	. 430	. 473	. 522	. 563	. 558	. 485	. 546	. 606
. 80	. 229	. 168	. 185	. 242	. 299	. 339	. 388	. 425	. 452	. 485	. 522	. 613
. 95	−. 012	−. 008	. 087	. 175	. 242	. 291	. 334	. 373	. 424	. 459	. 489	. 561
1. 08	--------	−. 041	. 007	. 080	. 142	. 187	. 239	. 291	. 329	. 371	. 415	. 495

DRAG COEFFICIENTS C_D

V/c	−4	−2	0	2	4	6	8	10	12	14	16	20
0. 50	0. 081	0. 072	0. 069	0. 070	0. 074	0. 081	0. 093	0. 105	0. 120	0. 139	0. 157	0. 198
. 65	. 091	. 080	. 072	. 071	. 076	. 083	. 095	. 106	. 130	. 186	. 207	. 272
. 80	. 103	. 089	. 094	. 102	. 113	. 125	. 142	. 161	. 181	. 203	. 224	. 281
. 95	. 149	. 143	. 139	. 142	. 147	. 155	. 165	. 181	. 201	. 221	. 245	. 299
1. 08	--------	. 160	. 155	. 152	. 156	. 164	. 173	. 183	. 199	. 217	. 238	. 285

AIRFOIL 3R20

LIFT COEFFICIENTS C_L

V/c	Angle of attack											
	−4	−2	0	2	4	6	8	10	12	14	16	20
0.50	0.275	0.309	0.363	0.399	0.442	0.489	0.534	0.564	0.624	0.687	0.749	0.635 .811
.65	.309	.313	.343	.388	.444	.481	.523	.417 .536	.443	.503	.566	.612
.80	.147	.103	.168	.230	.292	.327	.373	.411	.462	.518	.552	.627
.95	−.026	.010	.076	.160	.220	.269	.297	.344	.386	.428 .452	.464	.547
1.08	--------	−.057	.000	.059	.121	.179	.233	.260	.297	.332	.382	.464

DRAG COEFFICIENTS C_D

V/c	−4	−2	0	2	4	6	8	10	12	14	16	20
0.50	0.097	0.083	0.078	0.076	0.080	0.088	0.099	0.112	0.129	0.145	0.164	0.271
.65	.109	.092	.080	.078	.081	.089	.099	.148	.173	.200	.223	.279
.80	.118	.115	.115	.120	.131	.142	.157	.174	.192	.216	.243	.297
.95	.172	.167	.163	.165	.167	.177	.188	.199	.219	.240	.265	.316
1.08	--------	.183	.177	.175	.177	.181	.190	.205	.219	.236	.257	.300

AIRFOIL 4R8

LIFT COEFFICIENTS C_L

V/c	Angle of attack											
	−4	−2	0	2	4	6	8	10	12	14	16	20
0.50	0.047	0.105	0.171	0.234	0.290	0.345	0.403	0.453	0.500	0.562	0.594	0.704
.65	.059	.123	.184	.240	.295	.330	.395	.459	.511	.569	.606	.685
.80	.067	.134	.196	.242	.293	.347	.401	.459	.504	.538	.580	.664
.95	.048	.110	.166	.215	.265	.304	.346	.389	.446	.490	.537	.640
1.08	−.038	.024	.087	.145	.209	.250	.292	.333	.381	.421	.469	.556

DRAG COEFFICIENTS C_D

V/c	−4	−2	0	2	4	6	8	10	12	14	16	20
0.50	0.033	0.028	0.028	0.031	0.036	0.043	0.053	0.066	0.081	0.099	0.118	0.160
.65	.034	.029	.029	.031	.037	.044	.055	.068	.084	.103	.123	.192
.80	.038	.032	.031	.033	.037	.047	.059	.075	.095	.123	.153	.217
.95	.045	.038	.035	.038	.045	.056	.071	.091	.111	.137	.166	.230
1.08	.062	.054	.050	.051	.056	.064	.075	.090	.109	.130	.155	.214

AIRFOIL 5R8

LIFT COEFFICIENTS C_L

V/c	Angle of attack											
	−4	−2	0	2	4	6	8	10	12	14	16	20
0.50	0.037	0.095	0.157	0.225	0.294	0.346	0.400	0.450	0.502	0.552	0.593	0.671
.65	.051	.115	.175	.240	.303	.351	.385	.461	.514	.572	.622	.661
.80	.068	.133	.193	.241	.296	.356	.408	.467	.524	.571	.622	.674
.95	.044	.123	.191	.235	.296	.333	.371	.404	.473	.536	.578	.672
1.08	−.020	.042	.106	.165	.225	.267	.311	.361	.417	.466	.522	.614

DRAG COEFFICIENTS C_D

V/c	−4	−2	0	2	4	6	8	10	12	14	16	20
0.50	0.033	0.029	0.029	0.031	0.038	0.045	0.055	0.067	0.081	0.099	0.117	0.181
.65	.034	.029	.029	.032	.039	.046	.056	.069	.085	.102	.121	.196
.80	.037	.032	.031	.034	.040	.049	.061	.076	.094	.117	.143	.219
.95	.046	.037	.036	.038	.046	.056	.070	.089	.111	.135	.164	.231
1.08	.061	.053	.050	.050	.056	.064	.076	.092	.110	.133	.159	.227

Airfoil 6R8

LIFT COEFFICIENTS C_L

V/c	Angle of attack											
	−4	−2	0	2	4	6	8	10	12	14	16	20
0. 50	0. 000	0. 056	0. 119	0. 185	0. 262	0. 339	0. 412	0. 459	0. 496	0. 524	0. 596	0. 647
. 65	. 003	. 065	. 129	. 202	. 280	. 347	. 429	. 473	. 509	. 566	. 611	. 639
. 80	. 003	. 074	. 139	. 218	. 315	. 366	. 421	. 479	. 535	. 579	. 624	. 657
. 95	. 004	. 090	. 163	. 239	. 300	. 353	. 394	. 427	. 498	. 542	. 592	. 653
1. 08	−. 026	. 044	. 108	. 162	. 225	. 265	. 311	. 356	. 396	. 450	. 500	. 623

DRAG COEFFICIENTS C_D

V/c	−4	−2	0	2	4	6	8	10	12	14	16	20
0. 50	0. 037	0. 031	0. 030	0. 032	0. 037	0. 046	0. 059	0. 069	0. 082	0. 100	0. 119	0. 205
. 65	. 038	. 032	. 031	. 033	. 039	. 048	. 060	. 071	. 084	. 103	. 123	. 212
. 80	. 042	. 035	. 032	. 035	. 042	. 049	. 061	. 076	. 093	. 113	. 140	. 221
. 95	. 049	. 039	. 035	. 037	. 044	. 053	. 066	. 082	. 104	. 130	. 160	. 228
1. 08	. 062	. 052	. 047	. 047	. 051	. 058	. 068	. 081	. 099	. 121	. 147	. 220

Airfoil 4R16

LIFT COEFFICIENTS C_L

V/c	Angle of attack											
	−4	−2	0	2	4	6	8	10	12	14	16	20
0. 50	0. 176	0. 232	0. 302	0. 358	0. 416	0. 481	0. 524	0. 575	0. 635	0. 674	0. 721	0. 790
. 65	. 220	. 249	. 317	. 374	. 440	. 486	. 541	. 582	. 623	. 667	. 702	. 636
. 80	. 149	. 186	. 245	. 310	. 348	. 381	. 418	. 462	. 506	. 547	. 577	. 650
. 95	−. 064	−. 021	. 068	. 135	. 187	. 244	. 297	. 360	. 429	. 476	. 519	. 594
1. 08	--------	−. 036	. 020	. 080	. 130	. 190	. 240	. 283	. 324	. 377	. 428	. 470

DRAG COEFFICIENTS C_D

V/c	−4	−2	0	2	4	6	8	10	12	14	16	20
0. 50	0. 071	0. 063	0. 062	0. 064	0. 069	0. 078	0. 090	0. 102	0. 121	0. 133	0. 150	0. 188
. 65	. 079	. 069	. 066	. 067	. 072	. 080	. 091	. 103	. 117	. 131	. 149	. 222
. 80	. 088	. 075	. 070	. 071	. 074	. 082	. 095	. 114	. 135	. 162	. 188	. 247
. 95	. 123	. 111	. 106	. 105	. 107	. 116	. 128	. 143	. 163	. 184	. 207	. 263
1. 08	--------	. 132	. 124	. 121	. 122	. 127	. 136	. 148	. 163	. 181	. 202	. 242

Airfoil 5R16

LIFT COEFFICIENTS C_L

V/c	Angle of attack											
	−4	−2	0	2	4	6	8	10	12	14	16	20
0. 50	0. 017	0. 098	0. 186	0. 271	0. 354	0. 426	0. 508	0. 571	0. 622	0. 650	0. 701	0. 791
. 65	. 056	. 131	. 212	. 297	. 365	. 457	. 533	. 579	. 602	. 652	. 700	. 670
. 80	. 076	. 149	. 222	. 317	. 397	. 467	. 510	. 504	. 525	. 556	. 582	. 662
. 95	−. 052	. 013	. 107	. 164	. 221	. 263	. 310	. 361	. 400	. 467	. 526	. 574
												. 622
1. 08	−. 072	−. 012	. 047	. 108	. 169	. 224	. 278	. 320	. 362	. 413	. 449	. 514

DRAG COEFFICIENTS C_D

V/c	−4	−2	0	2	4	6	8	10	12	14	16	20
0. 50	0. 079	0. 070	0. 066	0. 066	0. 070	0. 078	0. 090	0. 106	0. 118	0. 128	0. 145	0. 190
. 65	. 080	. 070	. 066	. 066	. 071	. 080	. 094	. 104	. 113	. 130	. 150	. 219
. 80	. 093	. 081	. 075	. 074	. 076	. 081	. 091	. 107	. 132	. 159	. 184	. 242
. 95	. 117	. 104	. 100	. 098	. 102	. 109	. 122	. 139	. 158	. 180	. 204	. 259
1. 08	. 138	. 127	. 118	. 115	. 116	. 121	. 130	. 142	. 158	. 179	. 199	. 250

Airfoil 6R16

LIFT COEFFICIENTS C_L

V/c	Angle of attack											
	−4	−2	0	2	4	6	8	10	12	14	16	20
0. 50	−0. 049	0. 036	0. 112	0. 182	. 0275	0. 354	0. 431	0. 502	0. 579	0. 616	0. 672	0. 777
. 65	−. 038	. 052	. 126	. 211	. 293	. 366	. 455	. 515	. 575	. 629	. 680	. 771
. 80	. 000	. 086	. 172	. 242	. 334	. 386	. 462	. 510	. 543	. 554	. 590	. 675
. 95	−. 039	. 048	. 121	. 178	. 228	. 272	. 318	. 365	. 413	. 493	. 558	. 625
1. 08	−. 064	−. 005	. 052	. 109	. 158	. 215	. 256	. 298	. 334	. 377	. 421	. 529

DRAG COEFFICIENTS C_D

0. 50	0. 090	0. 080	0. 073	0. 069	0. 072	0. 078	0. 088	0. 097	0. 110	0. 122	0. 141	0. 185
. 65	. 093	. 081	. 073	. 070	. 073	. 079	. 089	. 094	. 108	. 124	. 145	. 191
. 80	. 100	. 087	. 080	. 075	. 070	. 074	. 085	. 100	. 118	. 143	. 171	. 228
. 95	. 112	. 101	. 095	. 092	. 093	. 099	. 112	. 127	. 148	. 169	. 193	. 246
1. 08	. 137	. 124	. 113	. 107	. 107	. 111	. 119	. 130	. 147	. 166	. 187	. 239

Airfoil C4

LIFT COEFFICIENTS C_L

V/c	Angle of attack											
	−4	−2	0	2	4	6	8	10	12	14	16	20
0. 50	−0. 048	0. 017	0. 075	0. 146	0. 209	0. 268	0. 327	0. 383	0. 440	0. 492	0. 527	0. 599
. 65	−. 048	. 014	. 082	. 151	. 210	. 271	. 338	. 390	. 452	. 496	. 548	. 599
. 80	−. 060	. 006	. 077	. 147	. 216	. 272	. 338	. 398	. 449	. 478	. 524	-------
. 95	−. 057	. 012	. 077	. 147	. 217	. 278	. 333	. 392	-------	-------	-------	-------
1. 08	−. 075	−. 001	. 060	. 126	. 173	. 243	. 300	-------	-------	-------	-------	-------

DRAG COEFFICIENTS C_D

0. 50	0. 013	0. 011	0. 010	0. 014	0. 021	0. 030	0. 042	0. 057	0. 086	0. 122	0. 160	0. 227
. 65	. 014	. 011	. 011	. 015	. 022	. 032	. 045	. 065	. 091	. 125	. 160	. 226
. 80	. 015	. 011	. 011	. 014	. 022	. 034	. 050	. 071	. 097	. 126	. 158	-------
. 95	. 021	. 014	. 013	. 017	. 025	. 038	. 056	. 078	-------	-------	-------	-------
1. 08	. 031	. 022	. 019	. 021	. 028	. 040	. 057	-------	-------	-------	-------	-------

Airfoil C8

LIFT COEFFICIENTS C_L

V/c	Angle of attack											
	−4	−2	0	2	4	6	8	10	12	14	16	20
0. 50	0. 026	0. 084	0. 148	0. 197	0. 255	0. 315	0. 373	0. 429	0. 466	0. 530	0. 594	0. 629
. 65	. 027	. 083	. 143	. 206	. 261	. 316	. 382	. 437	. 503	. 552	. 594	. 616
. 80	. 032	. 090	. 149	. 199	. 268	. 333	. 398	. 442	. 494	. 552	. 583	. 635
. 95	. 029	. 086	. 144	. 198	. 249	. 298	. 349	. 396	. 444	. 494	. 550	. 614
1. 08	−. 035	. 030	. 087	. 140	. 205	. 255	. 303	. 340	. 403	. 450	. 490	. 585

DRAG COEFFICIENTS C_D

0. 50	0. 017	0. 016	0. 017	0. 020	0. 027	0. 036	0. 047	0. 060	0. 074	0. 092	0. 111	0. 220
. 65	. 017	. 016	. 018	. 021	. 028	. 037	. 049	. 064	. 081	. 100	. 137	. 225
. 80	. 018	. 017	. 019	. 022	. 030	. 041	. 056	. 074	. 100	. 130	. 161	. 235
. 95	. 031	. 027	. 028	. 034	. 044	. 056	. 073	. 093	. 116	. 142	. 174	. 240
1. 08	. 046	. 041	. 040	. 044	. 052	. 063	. 076	. 094	. 116	. 141	. 169	. 237

Airfoil C12

LIFT COEFFICIENTS C_L

V/c	Angle of attack											
	−4	−2	0	2	4	6	8	10	12	14	16	20
0.50	0.099	0.146	.210	0.264	0.328	0.386	0.446	0.504	0.554	0.612	0.656	0.770
.65	.097	.152	.212	.272	.329	.389	.450	.502	.561	.598	.625	.684
.80	.108	.162	.224	.281	.330	.381	.419	.458	.498	.537	.574	.659
.95	.014	.074	.128	.180	.234	.289	.338	.388	.442	.482	.532	.620
1.08	−.058	−.004	.053	.118	.167	.227	.283	.324	.376	.425	.467	.564

DRAG COEFFICIENTS C_D

V/c	−4	−2	0	2	4	6	8	10	12	14	16	20
0.50	0.020	0.022	0.026	0.031	0.039	0.050	0.063	0.078	0.094	0.112	0.132	0.176
.65	.021	.023	.026	.032	.039	.051	.065	.079	.096	.115	.151	.223
.80	.028	.026	.029	.036	.045	.059	.080	.104	.129	.158	.186	.247
.95	.059	.056	.058	.064	.074	.088	.102	.124	.145	.167	.194	.258
1.08	.080	.074	.073	.076	.082	.094	.109	.126	.145	.167	.192	.252

Airfoil C16

LIFT COEFFICIENTS C_L

V/c	Angle of attack											
	−4	−2	0	2	4	6	8	10	12	14	16	20
0.50	0.165	0.212	0.271	0.333	0.388	0.440	0.502	0.539	0.603	0.648	0.719	0.816 .588
.65	.169	.225	.278	.325	.387	.442	.497	.555	.596	.519	.552	.668
.80	.169	.211	.238	.275	.316	.359	.401	.440	.459	.510	.534	.654
.95	−.035	.048	.117	.175	.233	.284	.334	.366	.418	.460	.518	.614
1.08	−.083	−.026	.025	.087	.145	.205	.267	.321	.360	.405	.443	.516

DRAG COEFFICIENTS C_D

V/c	−4	−2	0	2	4	6	8	10	12	14	16	20
0.50	0.027	0.031	0.037	0.044	0.053	0.064	0.079	0.095	0.112	0.130	0.150	0.243
.65	.029	.032	.038	.045	.054	.064	.078	.096	.111	.162	.186	.243
.80	.044	.043	.048	.061	.076	.093	.113	.135	.158	.182	.213	.267
.95	.094	.092	.093	.099	.108	.120	.136	.152	.172	.197	.222	.280
1.08	.118	.114	.113	.115	.120	.131	.142	.158	.176	.195	.216	.270

Airfoil C20

LIFT COEFFICIENTS C_L

V/c	Angle of attack											
	−4	−2	0	2	4	6	8	10	12	14	16	20
0.50	0.217	0.271	0.333	0.379	0.430	0.484	0.537	0.603	0.654	0.699	0.756	0.528
.65	.226	.279	.331	.380	.439	.483	.528	.398	.426	.457	.494	.555
.80	.090	.148	.188	.244	.294	.338	.379	.405	.438	.479	.527	.615
.95	−.059	.002	.098	.156	.236	.277	.312	.357	.405	.453	.478	.515
1.08	--------	−.066	−.017	.045	.109	.154	.203	.256	.300	.345	.395	.471

DRAG COEFFICIENTS C_D

V/c	−4	−2	0	2	4	6	8	10	12	14	16	20
0.50	0.038	0.043	0.050	0.058	0.068	0.078	0.093	0.114	0.130	0.148	0.167	0.278
.65	.042	.046	.051	.058	.069	.079	.092	.144	.175	.202	.225	.272
.80	.079	.081	.086	.097	.111	.129	.148	.165	.194	.210	.235	.289
.95	.134	.133	.133	.134	.143	.155	.168	.182	.203	.225	.249	.295
1.08	--------	.154	.150	.148	.152	.162	.174	.189	.204	.223	.245	.293

Reed Airfoil

LIFT COEFFICIENTS C_L

V/c	Angle of attack											
	−4	−2	0	2	4	6	8	10	12	14	16	20
0.50	0.071	0.135	0.194	0.257	0.305	0.363	0.421	0.468	0.528	0.575	0.618	0.687
.65	.081	.144	.200	.254	.313	.365	.424	.482	.544	.590	.638	.720
.80	.087	.150	.206	.266	.321	.378	.432	.480	.528	.568	.628	.738
.95	.038	.091	.139	.193	.240	.288	.337	.392	.436	.498	.564	.686
1.08	−.033	.028	.092	.145	.201	.241	.277	.323	.374	.429	.478	.581

DRAG COEFFICIENTS C_D

0.50	0.035	0.031	0.031	0.034	0.040	0.048	0.058	0.071	0.087	0.104	0.120	0.161
.65	.036	.032	.032	.035	.040	.049	.061	.074	.090	.107	.124	.170
.80	.041	.035	.035	.038	.044	.053	.066	.079	.096	.119	.143	.206
.95	.059	.053	.051	.053	.060	.068	.080	.096	.113	.137	.164	.229
1.08	.076	.068	.064	.063	.067	.074	.083	.098	.112	.133	.156	.216

Flat Plate Airfoil

LIFT COEFFICIENTS C_L

V/c	Angle of attack											
	−4	−2	0	2	4	6	8	10	12	14	16	20
0.50	−0.146	−0.071	−0.001	0.064	0.146	0.219	0.298	0.356	0.399	0.455	0.498	0.550
.65	−.155	−.080	.000	.080	.159	.231	.298	.341	.415	.450	.493	.540
.80	--------	−.084	.006	.095	.173	.245	.312	.369	.415	.449	.491	--------
.95	--------	−.112	.013	.110	.187	.257	.319	.373	.430	--------	--------	--------
1.08	--------	--------	.012	.105	.175	.244	.295	.351	.406	--------	--------	--------

DRAG COEFFICIENTS C_D

0.50	0.039	0.032	0.030	0.033	0.043	0.057	0.075	0.095	0.119	0.146	0.175	0.233
.65	.042	.033	.031	.034	.046	.059	.078	.099	.125	.150	.178	.230
.80	--------	.038	.034	.037	.050	.065	.085	.108	.128	.152	.180	--------
.95	--------	.043	.038	.044	.054	.069	.089	.112	.140	--------	--------	--------
1.08	--------	--------	.037	.044	.055	.069	.084	.105	.130	--------	--------	--------

Wedge Airfoil

LIFT COEFFICIENTS C_L

V/c	Angle of attack											
	−4	−2	0	2	4	6	8	10	12	14	16	20
0.50	−0.204	−0.140	−0.071	−0.004	0.064	0.129	0.200	0.272	0.339	0.416	0.487	0.562
.65	--------	−.142	−.073	−.008	.067	.129	.205	.279	.349	.412	.499	.574
.80	--------	--------	−.077	−.004	.072	.137	.216	.278	.373	.449	.496	.575
.95	--------	--------	−.078	−.003	.075	.146	.218	.302	.374	.456	.505	.581
1.08	--------	--------	−.063	−.004	.056	.120	.208	.288	.359	.431	.488	.564

DRAG COEFFICIENTS C_D

0.50	0.052	0.047	0.047	0.046	0.047	0.048	0.053	0.063	0.083	0.109	0.140	0.205
.65	--------	.050	.050	.051	.052	.052	.055	.066	.087	.113	.144	.209
.80	--------	--------	.053	.055	.055	.054	.059	.071	.091	.120	.148	.215
.95	--------	--------	.052	.054	.054	.057	.064	.077	.098	.124	.158	.227
1.08	--------	--------	.050	.049	.051	.056	.063	.076	.095	.121	.153	.220

Circular Arc Airfoil

LIFT COEFFICIENTS C_L

V/c	Angle of attack											
	−4	−2	0	2	4	6	8	10	12	14	16	20
0. 50	0. 064	0. 124	0. 179	0. 240	0. 300	0. 358	0. 397	0. 429	0. 483	0. 519	0. 564	0. 618
. 65	. 078	. 142	. 191	. 252	. 304	. 353	. 394	. 435	. 479	. 533	. 568	. 632
. 80	. 096	. 148	. 205	. 264	. 314	. 378	. 427	. 442	. 497	. 548	. 590	. 618
. 95	−. 002	. 057	. 115	. 173	. 238	. 295	. 388	. 421	. 483	. 532	. 572	. 616
1. 08	−. 034	. 031	. 094	. 144	. 189	. 233	. 301	. 368	. 418	. 476	. 521	. 615

DRAG COEFFICIENTS C_D

0. 50	0. 031	0. 028	0. 028	0. 031	0. 036	0. 045	0. 053	0. 064	0. 079	0. 097	0. 120	0. 204
. 65	. 028	. 028	. 028	. 031	. 037	. 046	. 053	. 064	. 080	. 098	. 122	. 208
. 80	. 033	. 029	. 029	. 032	. 039	. 049	. 058	. 065	. 081	. 101	. 125	. 214
. 95	. 049	. 041	. 038	. 039	. 043	. 051	. 064	. 073	. 086	. 109	. 136	. 218
1. 08	. 058	. 050	. 046	. 045	. 048	. 053	. 061	. 074	. 087	. 109	. 136	. 203

○

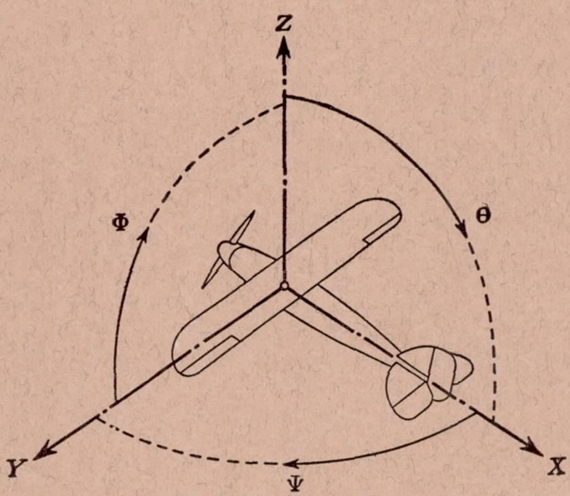

Positive directions of axes and angles (forces and moments) are shown by arrows

Axis		Force (parallel to axis) symbol	Moment about axis			Angle		Velocities	
Designation	Symbol		Designation	Symbol	Positive direction	Designation	Symbol	Linear (component along axis)	Angular
Longitudinal	X	X	rolling	L	$Y \longrightarrow Z$	roll	Φ	u	p
Lateral	Y	Y	pitching	M	$Z \longrightarrow X$	pitch	Θ	v	q
Normal	Z	Z	yawing	N	$X \longrightarrow Y$	yaw	Ψ	w	r

Absolute coefficients of moment

$$C_L=\frac{L}{qbS}\quad C_M=\frac{M}{qcS}\quad C_N=\frac{N}{qfS}$$

Angle of set of control surface (relative to neutral position), δ. (Indicate surface by proper subscript.)

4. PROPELLER SYMBOLS

D, Diameter.
p_e, Effective pitch
p_g, Mean geometric pitch.
p_s, Standard pitch.
p_v, Zero thrust.
p_a, Zero torque.
p/D, Pitch ratio.
V', Inflow velocity.
V_s, Slip stream velocity.

T, Thrust.
Q, Torque.
P, Power.
(If "coefficients" are introduced all units used must be consistent.)
η, Efficiency $= T\,V/P$.
n, Revolutions per sec., r. p. s.
N, Revolutions per minute., R. P. M.
Φ, Effective helix angle $=\tan^{-1}\left(\frac{V}{2\pi rn}\right)$

5. NUMERICAL RELATIONS

1 HP = 76.04 kg/m/sec. = 550 lb./ft./sec.
1 kg/m/sec. = 0.01315 HP.
1 mi./hr. = 0.44704 m/sec.
1 m/sec. = 2.23693 mi./hr.

1 lb. = 0.4535924277 kg.
1 kg = 2.2046224 lb.
1 mi. = 1609.35 m = 5280 ft.
1 m = 3.2808333 ft.